碩士學位論文

예열된 U-굽힘 고장력강의 롤 성형에 대한 매개변수 연구

濟州大學校 大學院

機械工學科

張 涯

2016年 8月

예열된 U-굽힘 고장력강의 롤 성형에 대한 매개변수 연구

指導敎授 鄭 東 垣

張 涯

이 論文을 工學 碩士學位 論文으로 提出함

2016年 6月

張涯의 工學 碩士學位 論文을 認准함

審査委員長 _____ ㊞

委　　員 _____ ㊞

委　　員 _____ ㊞

濟州大學校 大學院

2016年 6月

The Parametric Study of Preheated U-bending with High Strength Steel in Roll Forming Process

Ya Zhang
(Supervised by professor Dong-Won Jung)

A thesis submitted in partial fulfillment of the requirement for the degree of Master of Engineering

2016. 06.

This thesis has been examined and approved.

.....

Thesis director, Dong Won Jung, Prof. of Mechanical Engineering

.....

.....

.....

2016. 06.
Date

Department of Mechanical Engineering
GRADUATE SCHOOL
JEJU NATIONAL UNIVERSITY

JEJU NATIONAL UNIVERSITY

Contents

List of Figures ····· iii

List of Tables ····· vi

Summary ····· viii

Ⅰ. Introduction ····· 1

1.1 Overview of the roll forming process ····· 1

1.2 The purpose of the study ····· 4

Ⅱ. Experiment equipment and methods ····· 5

2.1 The Taguchi method ····· 5

2.2 The experiment machine for roll forming and pre-heating ····· 7

2.2.1 The material properties of the sheet ····· 7

2.2.2 The roll forming machine and forming rolls ····· 12

2.2.3 The heating devices and measurement tool for the spring back angles ····· 16

2.3 The calculation methods of roll forming process ····· 17

2.3.1 The calculation method of spring back angles ····· 17

2.3.2 The calculation method of bow defect ····· 19

Ⅲ. Results ····· 21

3.1 The COPRA simulation results ····· 21

3.1.1 The design of roll forming in COPRA ····· 21

3.1.2 The Taguchi method used in the simulation ····· 23

3.1.3 The optimization and analysis ····· 26
3.2 The ABAQUS simulation and experiment of spring back ····· 31
3.2.1 The spring back in ABAQUS simulation ····· 31
3.2.2 The experiment result and comparison ····· 37
3.3 The ABAQUS simulation of bow defect ····· 40
3.3.1 The Taguchi method used in the simulation ····· 40
3.3.2 The optimization and analysis ····· 47
3.4 The influence of pre-heating in roll forming process ····· 48
3.4.1 The simulation results of pre-heating with ABAQUS ····· 48
3.4.2 The experiment results of pre-heating ····· 55

Ⅳ. Conclusions ····· 68

References ····· 71

List of Figures

Fig. 1 The defects in the roll forming process ····· 3
Fig. 2 The material test under KSB08021 ····· 8
Fig. 3 The samples for the material test ····· 8
Fig. 4 The true strain-stress curve of SPFH590 ····· 9
Fig. 5 The true strain-stress curve of SPFH590 under 50 ℃ ····· 9
Fig. 6 The true strain-stress curve of SPFH590 under 150 ℃ ····· 10
Fig. 7 The true strain-stress curve of SPFH590 under 250 ℃ ····· 10
Fig. 8 The true strain-stress curve of strainless steel. ····· 11
Fig. 9 The true strain-stress curve of mild steel. ····· 11
Fig. 10 The layout of the roll forming machine ····· 12
Fig. 11 The roll forming machine ····· 13
Fig. 12 The roll dimension of the roll forming machine ····· 15
Fig. 13 The heating device of the pre-heating process ····· 16
Fig. 14 The protractor ····· 16
Fig. 15 The measured lines of spring back angles in ABAQUS ····· 18
Fig. 16 The definition of bow displacement ····· 19
Fig. 17 Bow defect measuring along the path in the simulation ····· 20
Fig. 18 The flower design of the sheet ····· 22
Fig. 19 The spring back angle in COPRA ····· 27
Fig. 20 The parameter levels of the factors ····· 28
Fig. 21 The strain distribution of the sheet after roll forming process ····· 29
Fig. 22 The plastic strain distribution of the sheet after roll forming process

..... 30
Fig. 23 The assembly of the roll forming process 34
Fig. 24 The mise stress distribution of the sheet with high strength steel ... 35
Fig. 25 The mise stress distribution of the sheet with strainless steel 35
Fig. 26 The mise stress distribution of the sheet with mild steel 36
Fig. 27 The spring back angles of different materials 36
Fig. 28 The experiment results of the three kinds of materials 37
Fig. 29 The bow displacement in the simulations 44
Fig. 30 The longitudinal strain along the edge of the sheet 45
Fig. 31 The longitudinal strain along the centerline of the sheet 46
Fig. 32 The parameter levels of the bow defect 47
Fig. 33 The spring back measured in ABAQUS with different temperature · 49
Fig. 34 The bow defect measured in ABAQUS with different temperature ... 50
Fig. 35 The forming force under room temperature 51
Fig. 36 The forming force under 50 ℃ 51
Fig. 37 The forming force under 150 ℃ 52
Fig. 38 The forming force under 250 ℃ 52
Fig. 39 The internal energy of the SPFH5590 under different temperature ...
..... 53
Fig. 40 The kinetic energy of the SPFH5590 under different temperature 53
Fig. 41 The pre-heating locations of the experiments 57
Fig. 42 The pre-heating height of the butane torch 58
Fig. 43 The butane torch setting in the forming process 59
Fig. 44 The experiment results of high strength steel with pre-heating 60
Fig. 45 The experiment results of strainless steel with pre-heating 61
Fig. 46 The experiment results of mild steel with pre-heating 62
Fig. 47 The spring back angles of different pre-heating locations with high strength steel 63
Fig. 48 The spring back angles of different pre-heating locations with

strainless steel ····· 64
Fig. 49 The spring back angles of different pre-heating locations with mild steel ····· 65
Fig. 50 The bow displacement of different materials ····· 66

List of Tables

Table 1 The orthogonal array ····· 6
Table 2 The mechanical property of material ····· 7
Table 3 Process parameters and three levels ····· 23
Table 4 The orthogonal array of COPRA simulation ····· 24
Table 5 Comparison of measured roughness data of spring back angles ····· 25
Table 6 The comparison of spring back angles ····· 39
Table 7 Process parameters and three levels ····· 40
Table 8 The orthogonal array of ABAQUS simulation ····· 42
Table 9 Comparison of measured roughness data of bow defect ····· 43
Table 10 The experiments with pre-heating ····· 56

SUMMARY

With the development of the automotive industry, the automotive industry put forward a new appeal of safety, environmental protection and energy saving. The emergence of high-strength steel meets the requirement of those highly impact factors. High strength steel can achieve the same strength as well as effectively reduce the material thickness. High strength steel forming technique has been widely recognized on the market, so the insiders pay close attention to this technology. However, with the increase of strength, the elongation and plastic property of the sheet have been reduced, the forming performance decreased and more difficult to make deformation at room temperature. At the same time, because of the work hardening, the product is easy to crack and have a large spring back angle. To solve this problem, some researchers come up a method to apply the heating process to the sheet before the forming process. With the pre-heating process, the microstructure of the steel has been changed, thereby affecting the phatic property and the elongation of the sheet, reduce the deformation resistance and make the sheet easier to deform.

Roll forming is a kind of plastic forming process in which a steel strip is bent by several sets of rolls gradually into the desired shape. The products are cold roll forming steels with various sections. Roll forming is one of the most widely used processes in the world for forming metal. Roll forming is a complex deformation process, which involves large displacement, finite strain and the problems of contact and friction between strip and rolls. This process exhibits obvious geometry, physical and boundary nonliterary. The complex processes contain many aspects such as geometry, kinematics and dynamics,

etc. The forming process involves not only transverse bending, but also other additional deformations.

In this paper, we have set up two kinds of roll forming models with the high strength steel using ABAQUS software which are cold roll forming and preheated roll forming. The sheets in both two models have been measured the contour bow defect of displacement and the stress are used to analysis the deformation of the sheet. The spring back also has been developed in the two simulations. At last, experiments were carried out to verify the validity of the proposed models.

Ⅰ. Introduction

1.1 Overview of the roll forming process

The sheet after roll forming also have defects such as buckling, spring back, wave, bow and so on. Some defects have been shown in the Fig.1. Those defects are affected by many forming parameters and sometimes they are depending on the combination of several factors [1-3]. Compared to other forming technology, roll forming has the advantage of high production effectiveness, low cost and easier to get a complicated cross-sectional profiles. Usually roll forming is at room temperature, the roll forming also called cold roll forming.

Roll forming production line is more effective and the process is continuous which also make it has a higher economy. The length of the sheet can be adjusted without to having to replace the rolling tool. Compared with the stamping and bending process, roll forming is more flexible, especially for the small-scale production. Traditional molding and other produce any cross-sectional profiles, while punching and bending section to produce only relatively simple [4-9].

The most important advantage of cold-formed profiles is relatively uniform hardening properties and high surface quality, plated metal and enamel processed substantially without leaving scratches.

Cross-section cold-formed steel is widely used in various industrial fields, especially automobile manufacturing and construction, the traditional cold-formed profiles or closed beam-like openings in high demand.

G. Nefussi and P. Gilormini [10] have applied a kinematical approach in the paper for predicting the optimal shape and the deformed length of a metal

sheet during cold-roll forming. Tao Zhou and Zhao Yang [11] has analyzed the influence of final rolling speeds varying from 0.1 m/s to 0.4 m/s on the microstructure, textures, mechanical properties and stretch formability of AZ31 alloy sheet rolled at 550 ℃.

In 2004, A. Alsamhan, I. Pillinger and P. Hartely [12] applied remeshing techniques to the roll forming process with the sheet friction calculation.

Zhang Dongjuan and Cui Zhenshan [13] had developed an analytical model for predicting the sheet spring back after U-bending based on the Hill's 48 yield criterion and plane strain condition. Also three materials hardening - kinetic, isotropic and combined hardening has been used to consider the effect in the bending process.

R. Safdarian and H. Moslemi Naeini [14] studied the effect of some roll forming parameters of channel section are investigated on the edge longitudinal strain and bow defect of products. The relationships between the parameters and defect have been recovered with simulation and experiment method.

Sukmoo Hong and Seungyoon Lee [15] have design a roll forming simulation with the simulation program (COPRA FEA-RF). The influences of some factors on the forming length decisively have been analyzed and the sensitivity of these factors have been considered. At last, the experiments have been set up to verify the simulations.

Vitalii Vorkov and Richard Aerens [16] studied the spring back of different types of high-strength steels using finite element modeling. The shell element and solid element had been compared and the deflection of the sheet during and after bending had been measured according to the images record by a camera.

Some defects [17] in the roll forming have been shown in the Fig. 1. The bow defect and twist defect are caused by the non-uniform transversal distribution of the longitudinal membrane strain, or in other words, the

non-uniform longitudinal elongation and shrinkage of the strip. This nonconformity is one of the fundamental characteristics of deformation of the strip during roll forming.

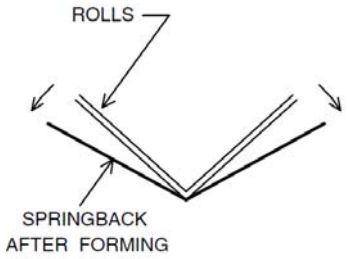

(a) Spring back defect

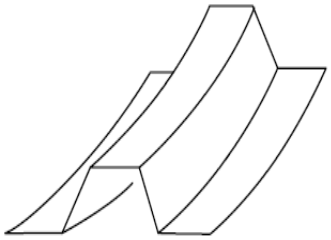

(b) Bow defect

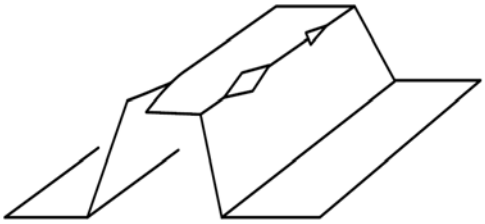

(c) Crack defect

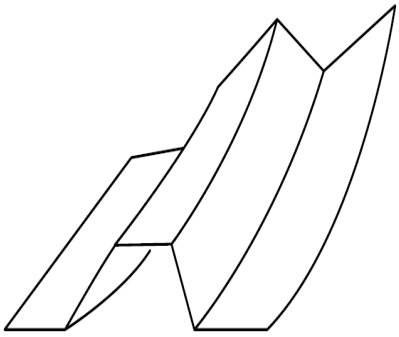

(d) Twist defect

Fig. 1 The defects in the roll forming process

1.2 The purpose of the study

The elastic-plastic method and the sheet forming in roll forming process are so complicated and it is difficult to work out the stress and strain distribution and other parameters. Only with the theoretical derivation and analysis are extremely difficult to get the results and it will take a lot of time. The finite element method has provided a reasonable way to this by dividing the sheet metal into a small element and calculating the results part by part. Through a mass of simplifications and assumptions, the forming process has been simulated and calculated.

In this paper, we are mainly focus on analysis the cold roll forming defects under different conditions. Flower design of the sheet has been done with the COPRA software. The COPRA software has been used to analyze the influence of the factors on the spring back defect. By analysis the results we intend to find out the most sensitive factor for the spring back defect and make optimizations.

Also, we have established a number of simulations in ABAQUS software in order to get the result of the spring back with different materials. There are three materials used in the simulation and three experiments have been set up under the same conditions to verify the simulation results. At last, the simulation results have been compared with the experiment results. Also, the theoretical spring back angle has been calculated and compared with the simulations and experiments.

Besides, the bow defect has been learned in the paper. The Taguchi method has been used to optimize the bow defect with ABAQUS software.

Based on the results above, we analyze the bow defect and spring back with the pre-heating process. The simulation and experiment have been set up to study about the influence of the temperature on spring back and bow defect.

Ⅱ. Experiment equipment and methods

2.1 The Taguchi method

The object of this study is to minimize the defects in the roll forming process. The Taguchi method [18] is one of the most well-known methods of robust design. The Taguchi method can optimize the defect in a simple and efficient way. The Taguchi method employs generic signal-to-noise (S/N ratio) ratio to quantify the quality of the products and process designs.

If three levels for each of the three factors are considered, a total of 27 (3^3) combinations is required. By using the Taguchi method to simplify the experiment numbers and save calculation time, the orthogonal array L9 (3^3) have been used as shown in Table 1.

We can determine the effect of each factor with Signal-to-Noise ratio (S/N ratio). Depending on the object of the experiment, different S/N ratio may be applicable. Depending on the object of the experiment, different criterion may be suitable for the results. There are two kinds of criterion in the Taguchi method. As shown in Eq. (1) and Eq. (2) are the formulas for the two criterion and Eq. (1) is for the "smaller is better", Eq. (2) is for the "bigger is better". For this study of spring back angle in the U-bending process, the criterion is "smaller is better". The S/N ratio formula is shown on Eq. (1).

$$S/N = -10\log_{10}\left[\frac{1}{n}\sum_{i=1}^{n} y_i^2\right] \tag{1}$$

$$S/N = -10\log_{10}\left[\frac{1}{n}\sum_{i=1}^{n}\frac{1}{y_i^2}\right] \tag{2}$$

In the formula, the n is the number of experiments or simulation repetitions, yi is the simulation or experiment result, and i stand for the number of design parameters arranged in the Taguchi orthogonal array (OA).

With the S/N ratio result of each experiment, we can evaluate the quality of the design solution and calculate out the best combination of the factors and levels.

Table 1 The orthogonal array

Experiment No.	Parameter Levels			Experiment Conditions
	A	B	C	
1	1	1	1	A1 B1 C1
2	1	2	2	A1 B2 C2
3	1	3	3	A1 B3 C3
4	2	1	2	A2 B1 C2
5	2	2	3	A2 B2 C3
6	2	3	1	A2 B3 C1
7	3	1	3	A3 B1 C3
8	3	2	1	A3 B2 C1
9	3	3	2	A3 B3 C2

2.2 The experiment machine for roll forming and pre-heating

The experiment used the roll forming machine to investigate the forming result with the heating process. The roll forming machine has four stands and driven by a motor. The sheet passes through the rolls and deform into the shape we desired.

2.2.1 The material properties of the sheet

There are three kinds of materials used in the current work. The mechanical properties of the material have been tested by the standard of KSB0802. Fig. 2 shows the material test process.

The material used in this simulations and experiments are SPFH590, strainless steel and mild steel. The material samples have been shown in Fig. 3.The mechanical property of the materials have been shown in Table 2. The true strain-stress curves have been shown from Fig. 4 to Fig. 9.

Table 2 The mechanical property of the materials

	Yield strength (MPa)	Ultimate tensile strength (MPa)	Young's Modulus of elasticity (GPa)	Poisson's ratio	Elongation (%)
SPFH 590	448	671	250	0.29	25
Strainless steel	251	340	250	0.30	46
Mild steel	205	520	250	0.30	50

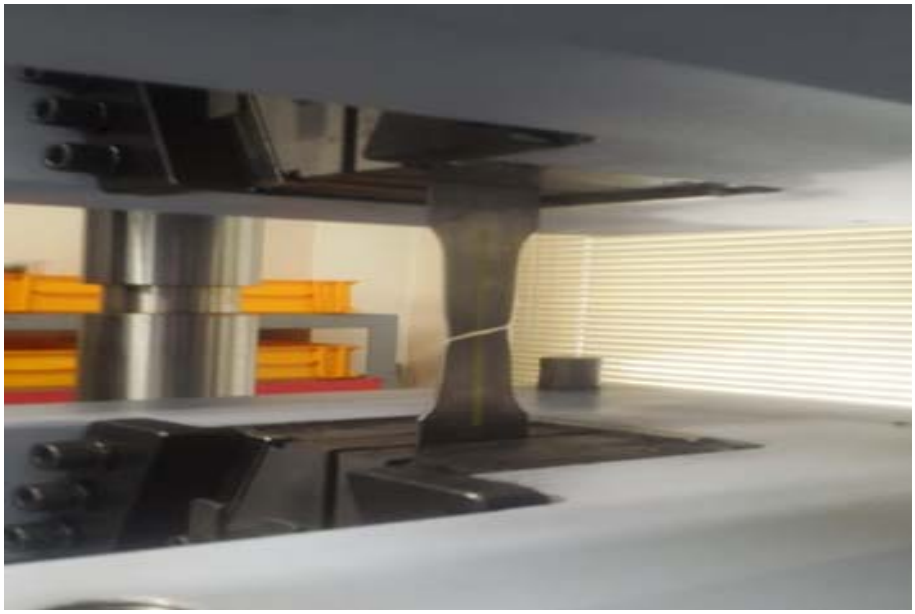

Fig. 2 The material test under KSB0802

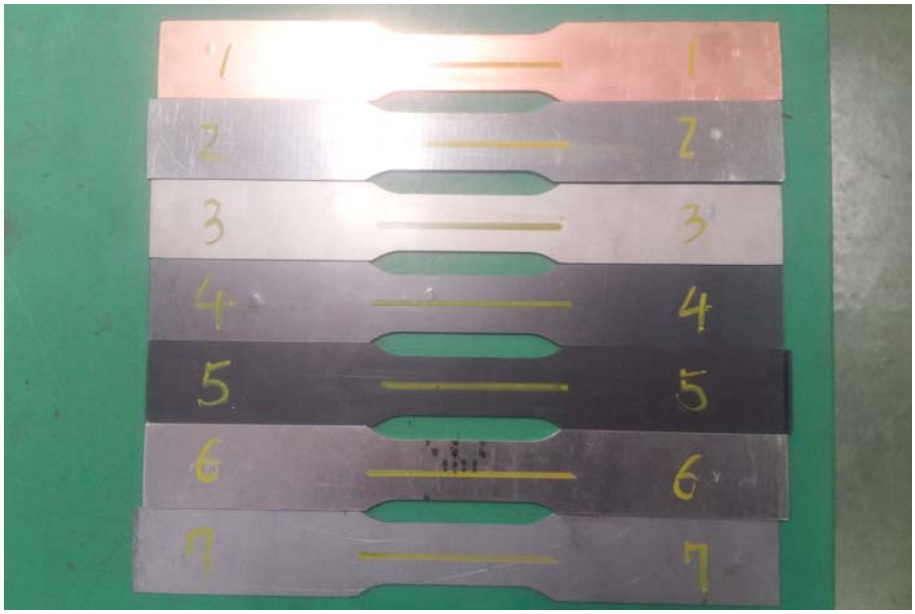

Fig. 3 The samples for the malarial test

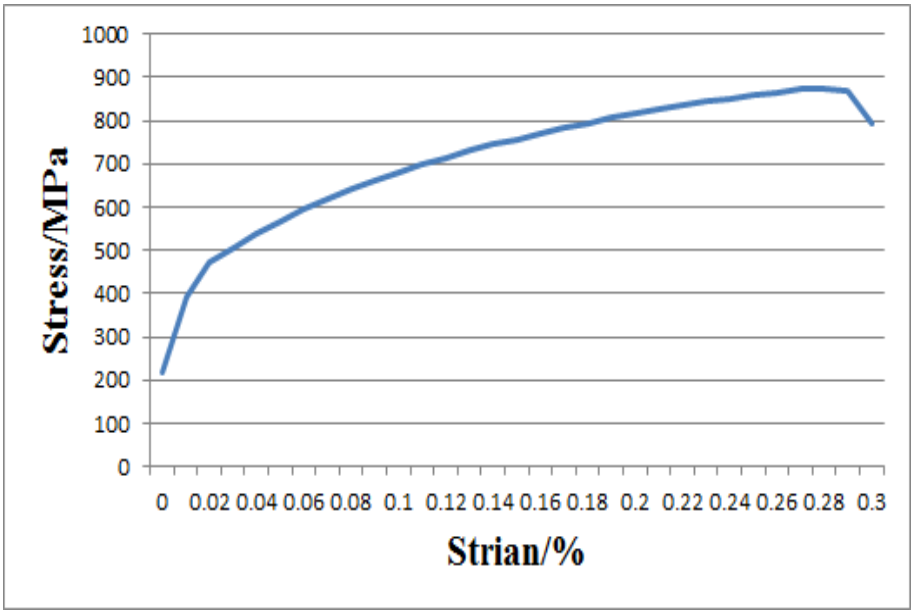

Fig. 4 The true stain-stress curve of SPFH590

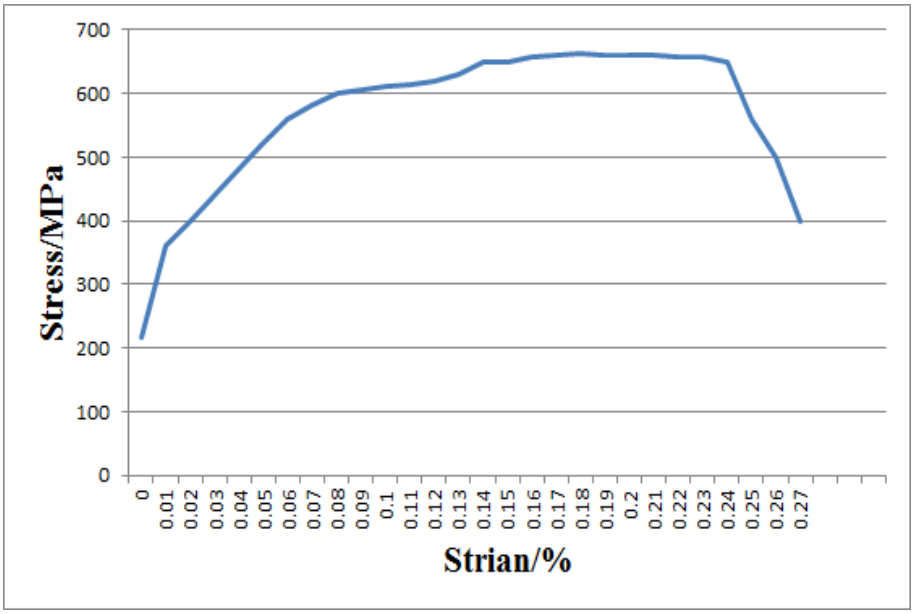

Fig. 5 The true strain-stress curve of SPFH590 under 50 ℃

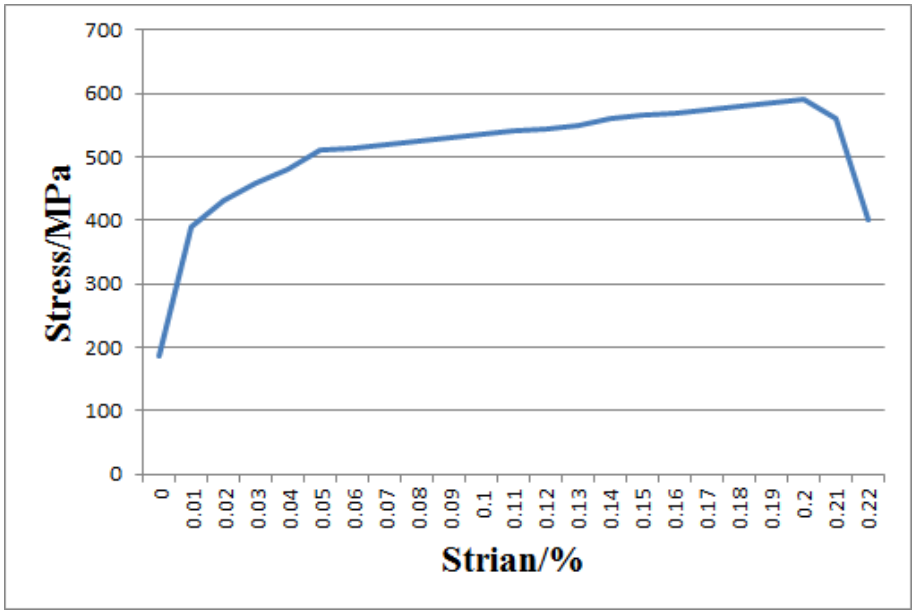

Fig. 6 The true strain-stress curve of SPFH590 under 150 ℃

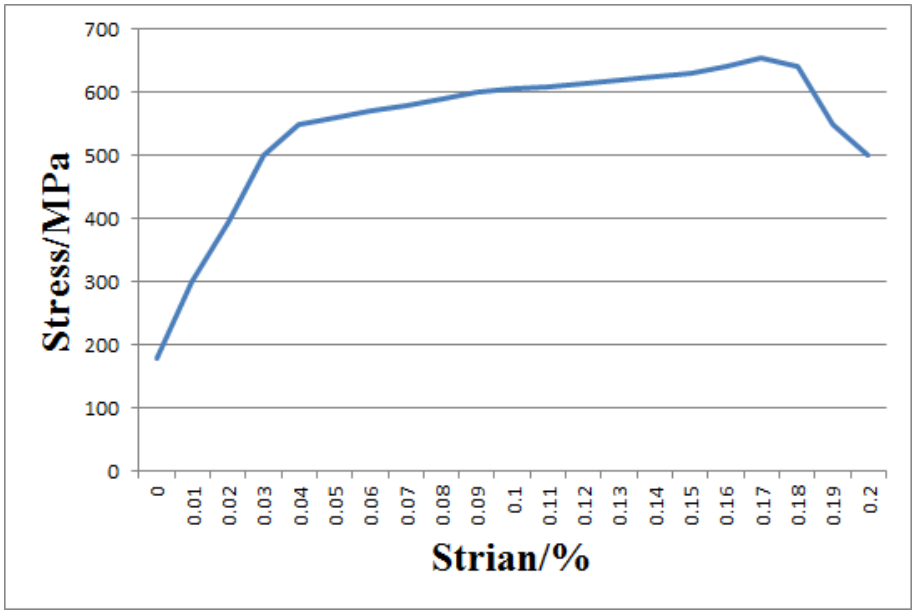

Fig. 7 The true strain-stress curve of SPFH590 under 250 ℃

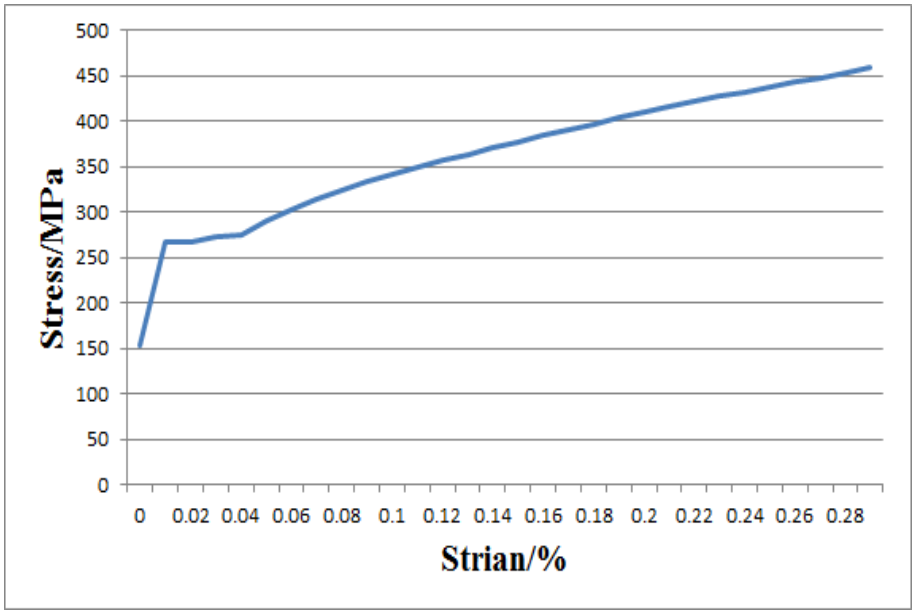

Fig. 8 The true strain-stress curve of strainless steel

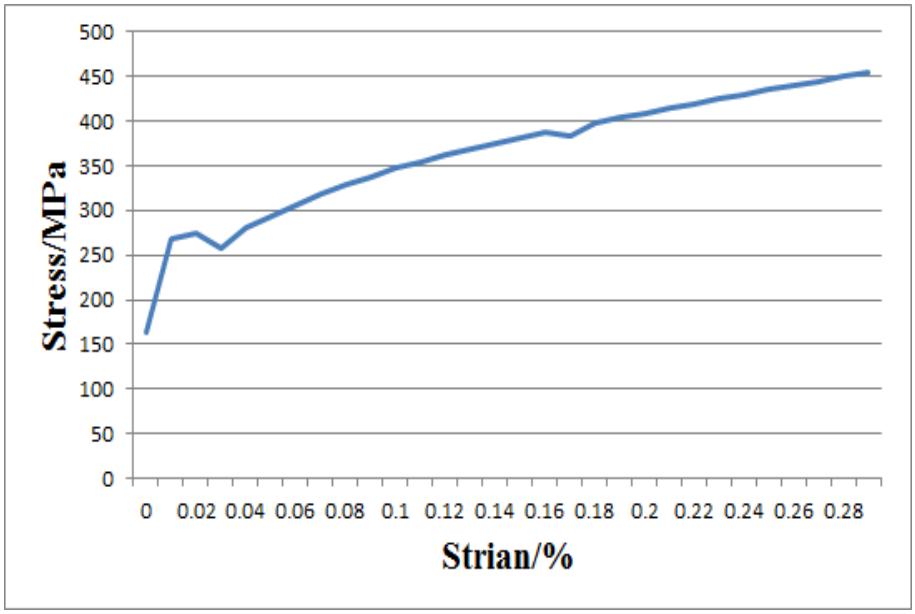

Fig. 9 The true strain-stress curve of mild steel

2.2.2 The roll forming machine and forming rolls

The roll forming machine layout has been shown in Fig. 10. The dimensions of the machine have been demonstrated on the figure. The roll forming machine include four stands and driven by a motor inside the machine. Every stand has two mills and the upper roll is adjustable and low roll is fixed. The gap is controlled by the screw bolt and springs over the stand. In this way, the gap between the rolls can adapt to the thickness of sheet and other forming conditions. There is an entry guide before the forming stands to make the sheet forming in a line.

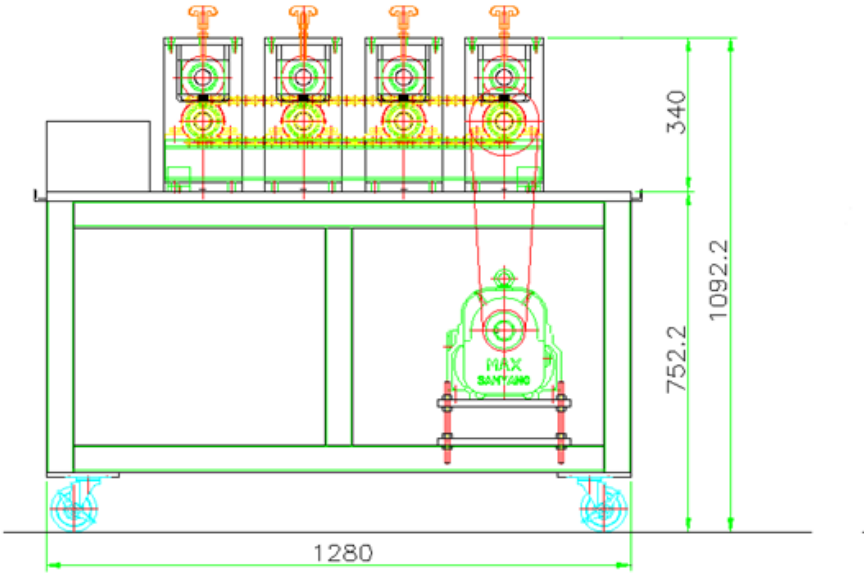

Fig. 10 The layout of the roll forming machine

Fig. 11 shows the roll forming machine used in the experiment. The rolls connect each other by the chain and the velocity is controlled by the panel. Fig. 12 shows the dimensions of the U-bending roll dies. There are four groups of rolls and the deformation angle of each stand is 22.5 °, 45 ° 67.5 ° and 90 °. The forming angle of lower roll is smaller than we design is due to the metal flow in the forming process. Considering the shape of the sheet, the scoring rolls and flattener are not necessary for this roll forming process. With this design, the forming angle after U-bending process will be 90 ° ideally.

Fig. 11 The roll forming machine

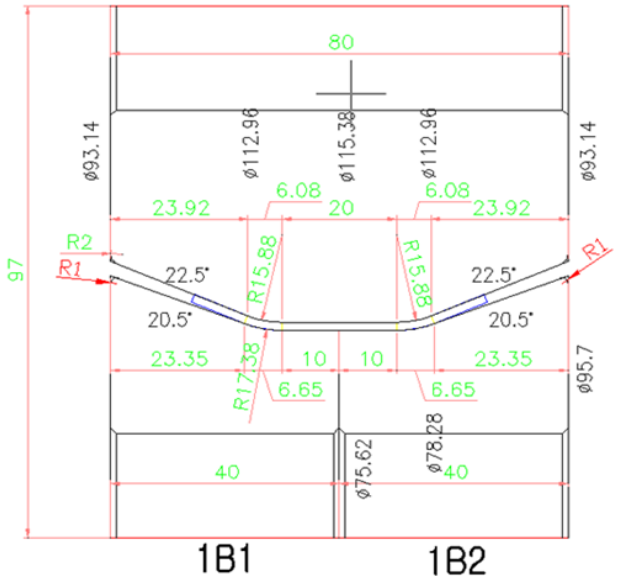

1T

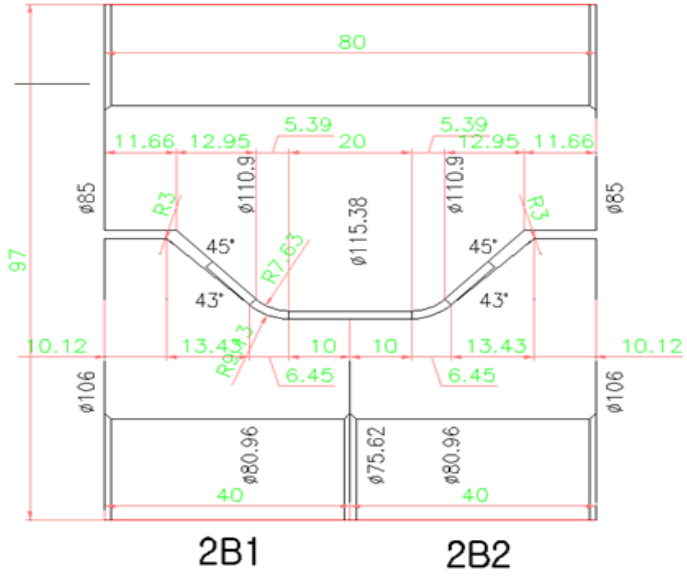

2T

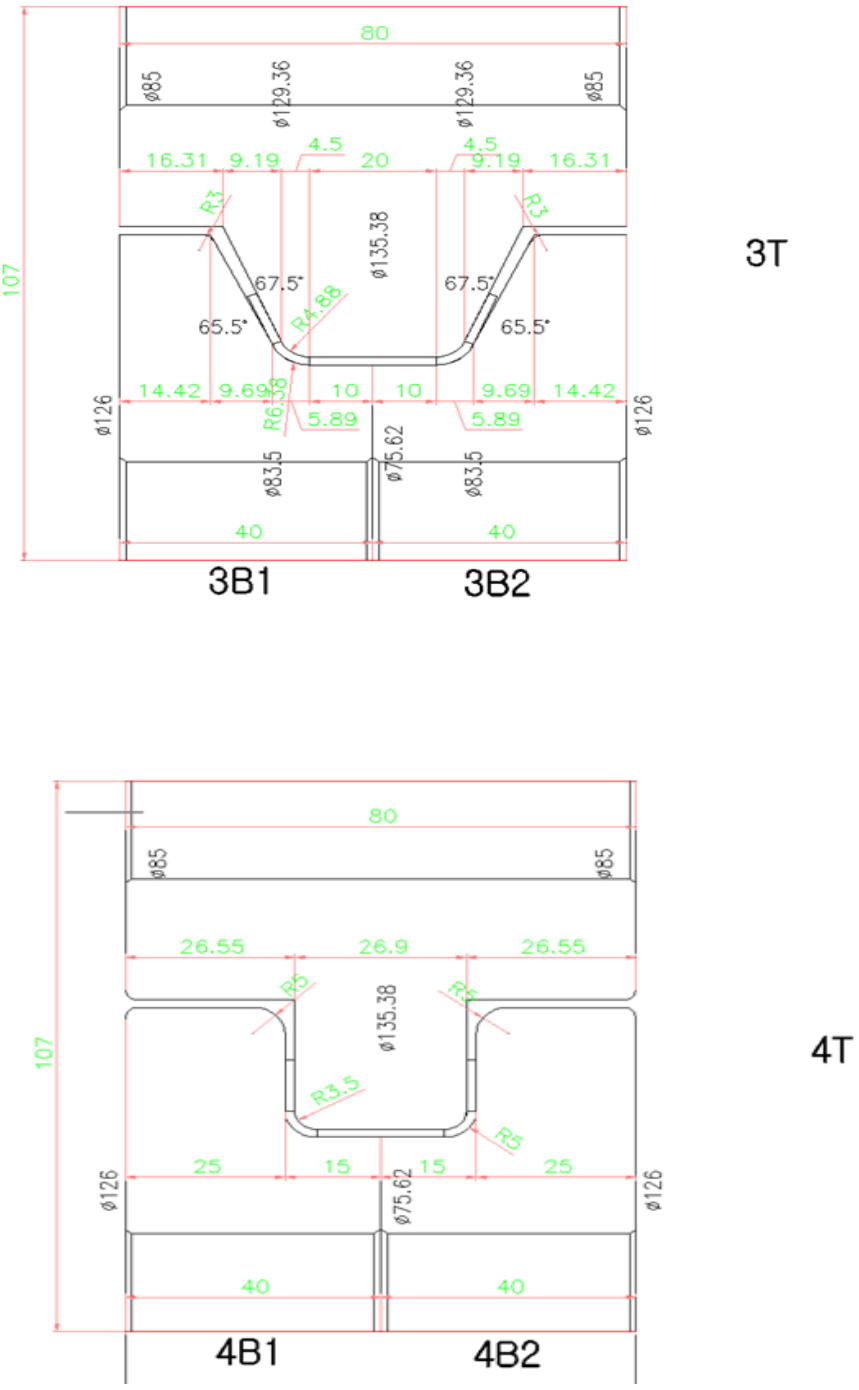

Fig. 12 The roll dimension of the roll forming machine

2.2.3 The heating devices and measurement tool for the spring back angles

The heating devices used in this experiment have been shown in Fig. 13. The sheet is heated by a butane gas torch. The heating devices have been fixed in the frame above the roll forming machine. The height of the flame is 800 mm and the height of the flame is 70 mm. As shown in the Fig. 14, the angle is measured by a protractor. With this we can calculate out the bending angle and then we can know the spring back angle.

Fig. 13 The heating device for the heating process

Fig. 14 The protractor

2.3 The calculation methods of the roll forming

In this study, we are focusing on the forming defect of spring back and bow. This two defects are the main defects in the roll forming process and easily occurred with the redundant deformation. The spring back defect is calculated by the angle between the desired angle and angle after spring back. The bow defect has been calculated with the maximum displacement in the centerline of the sheet.

2.3.1 The calculation method of spring back angles

The spring back angle in the ABAQUS was by measuring the angle of the slicing line. As show in Fig. 15, we slice the sheet into 8 parts. The spring back angles at the start point and end point are not accurate enough because of the sudden change of force and deformation. In general, the amount of spring back deformation at the entry and exit ends of cutoff metal sheet is larger than that of the midpoint. We measure the five slices in the middle of the sheet to get the spring back angles.

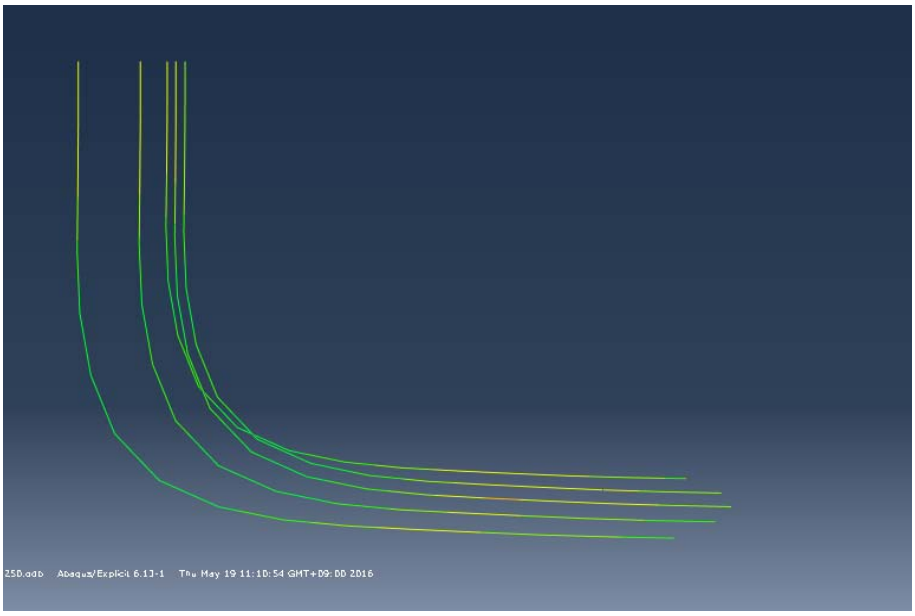

Fig. 15 The measured lines of spring back angle in ABAQUS

2.3.2 The calculation method of bow defect

Fig. 16 shows the bow displacement in the roll forming process. Bow is the sheet curved in the vertical direction. Usually bow can be measured in two ways, one is the radius of the curve and another one is the displacement of the curve. In this paper, we used the second method to evaluate the bow curve. The displacement distance has been defined to be the maximum displacement in the vertical direction. As shown in Fig. 17, the bow defect measured in the simulations was defined by a path. The path is in the middle of the sheet channel section along the strip length. The coordinate of the point on the path have been measured with the ABAQUS software. In this way, we can know the bow displacement of the sheet.

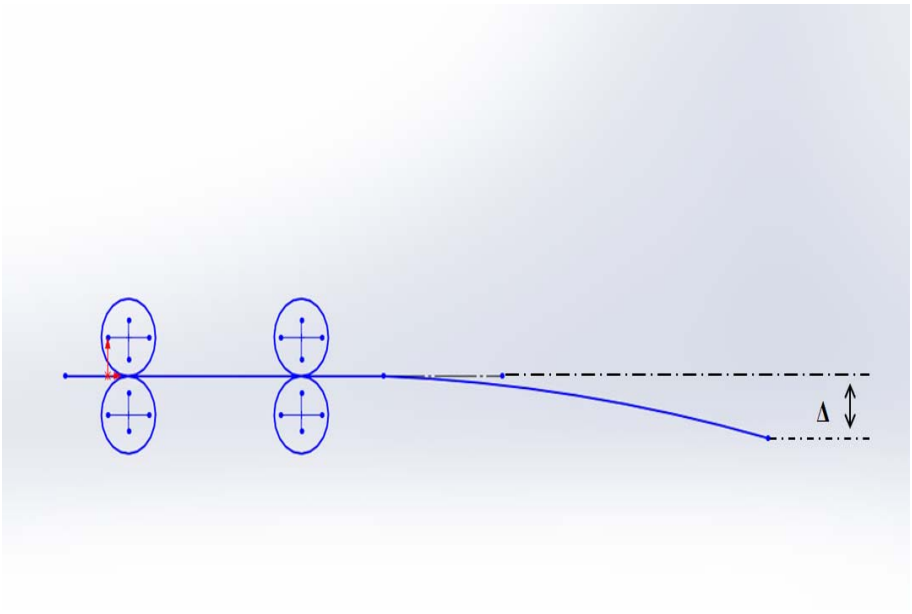

Fig. 16 The definition of bow displacement

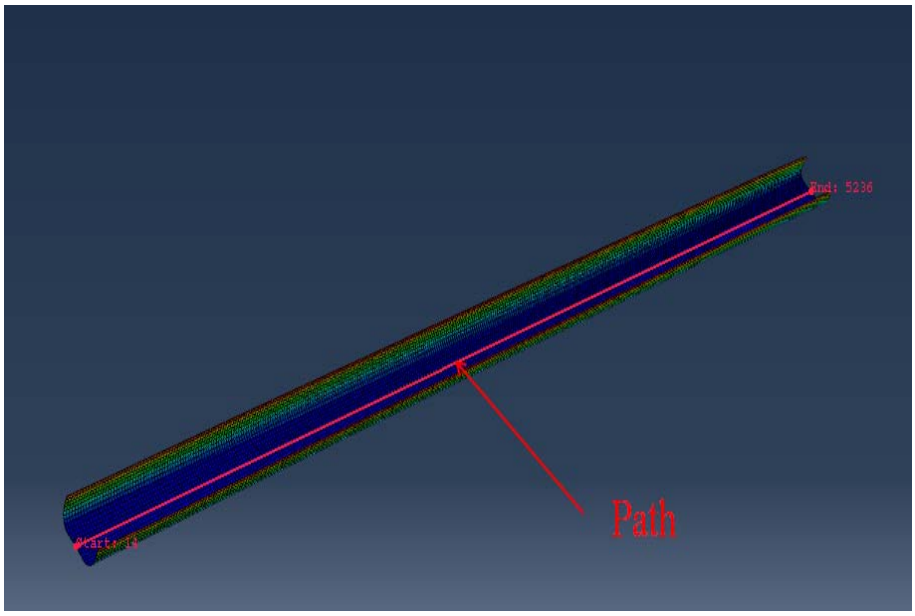

Fig. 17 Bow defect measuring along the path in the simulations

Ⅲ. Results

3.1 The COPRA simulation results

COPRA is one of the most convenient software to design the roll forming process. The software can help engineers to design the roll forming process in a more professional way and make the work simpler. With the software, the design and manufacturing cost can be reduced. The software offers a group of tools from roll flower design to roll design and the roll forming simulation. From which we can get the stress and strain distribution of the sheet and help engineer to optimize the design.

A U-bending process has been developed in this simulation with the COPRA software to reveal the relationship between the spring back angle and roll forming parameters.

The material investigated in this simulation is SPFH590 which is a kind of high strength steel. The Young's module is 70500 N/mm^2, the yield point is 110 N/mm^2. The roll forming process has been designed to be four stages and the deformation angle with each stage is constant to be 22.5 °.

3.1.1 The design of the roll forming in COPRA

The flower design has been shown in Fig. 18. There totally 4 passes in the forming process. For each pass have a constant bending angle with 22.5 degrees. The unfolding plane is defined to be in the center of the sheet. The strip width is calculated with BIN 6935. The distance between the stands is constant to be 220 mm.

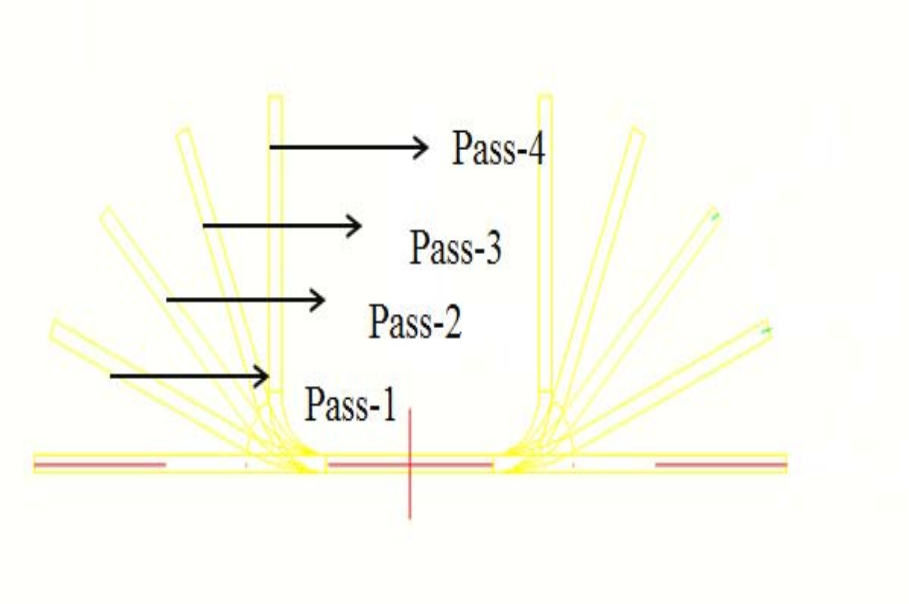

Fig. 18 The flower design of the sheet

3.1.2 The Taguchi method used in the simulations

The dimension of the sheet in this simulation is designed to be 100 mm width and 300 mm in longitude. The simulation calculation method is Hauschild's statement and the exponent is 2.5. The number of the surface element along the axis is 32 and cross axis is 14. The sheet is varied in many types based on three different thicknesses (1, 2 and 3 mm), three different radiuses (1.5, 2.5 and 3.5 mm) and three different widths (20, 40 and 60 mm). The roll forming process is at room temperature and the roll velocity is not considered in this process.

To conduct the optimization, there are three factors have been applied to the simulations which were the width of the U-bending, radius of the rolls and sheet thickness as shown in Table 3.

Table 3 Process parameters and there levels

Symbol	Factor	Unit	Level 1	Level 2	Level 3
A	Flange Width	mm	10	15	20
B	Thickness	mm	1	2	3
C	Radius	mm	1.5	2.5	3.5

For three levels with three factors, there will be totally 27 combinations need to be required. However, considering about the time while the effect of each factor, the orthogonal array L3 (3^3) has been chosen to arrange the simulations. The combination of the simulations is listed in Table 4. There will be 9 groups of simulations with different factors and different levels.

The S/N ratio and spring back angle is calculated in each simulation as shown in Table 5. According to the criterion "smaller is better", the corresponded S/N ratio shows that the optimum experiment is experiment 2 with A1, B3 and C3. The minimum spring back angle will be 1 degree.

Table 4 The orthogonal array of COPRA simulation

Simulation No.	Parameter Level		
	A	B	C
	Flange Width (mm)	Thickness (mm)	Radius (mm)
1	1	1	1
2	1	2	2
3	1	3	3
4	2	1	2
5	2	2	3
6	2	3	1
7	3	1	3
8	3	2	1
9	3	3	2

Table 5 Comparison of measured roughness data of spring back angles

Simulation No.	Parameter Levels				Calculated S/N ratio ration for spring-back (DB)
	A (mm)	B (mm)	C (mm)	Maximum spring back angle (°)	
1	10	1	1.5	1.29	-2.21
2	10	2	2.5	1.18	-1.43
3	10	3	3.5	1.15	-1.21
4	15	1	2.5	1.74	-4.81
5	15	2	3.5	1.39	-2.86
6	15	3	1.5	0.96	0.35
7	20	1	3.5	2.20	-6.85
8	20	2	1.5	1.00	0
9	20	3	2.5	0.03	30.46

3.1.3 The optimization and analysis

The effects of the factors on the spring back were evaluated in Fig. 20. As a result of the application of Taguchi method, the optimum levels of the factors were A1, B2 and C1. The spring back angle after optimization is 1.29 degree as showed in Fig. 19. This result is obviously larger than the combination simulations we did. This is because the factor we considered is not enough.

These factors have no significant influence on the spring back. Which means more factors and combinations need to apply to the optimization process. Factors such as forming gap, inner distance of stand and roll dimension also can affect the spring back.

Fig. 21 shows the strain distribution of the sheet after roll forming with the optimized factors. We can found that the strain of the sheet is up to 2.3% and thus too high. The strain decreased with the roll forming process. The strain in this simulation is much higher than the limitation and may result in many defects. Either the roll stands should increase or the roll dimension should modify. The plastic strain distribution is shown on Fig. 22. The plastic strain increased with the forming process. The strain of side 2 is bigger than side 1.

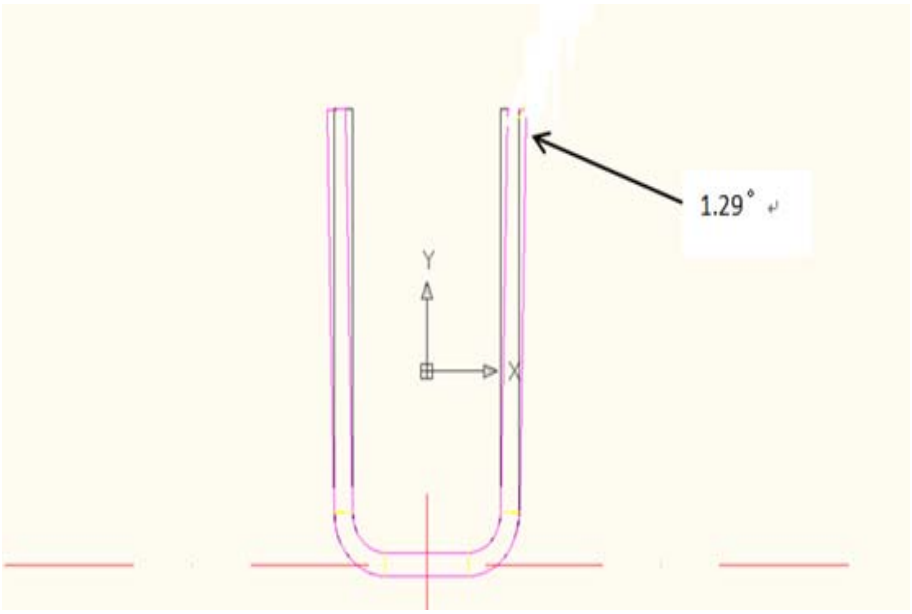

Fig. 19 The spring back angle in COPRA

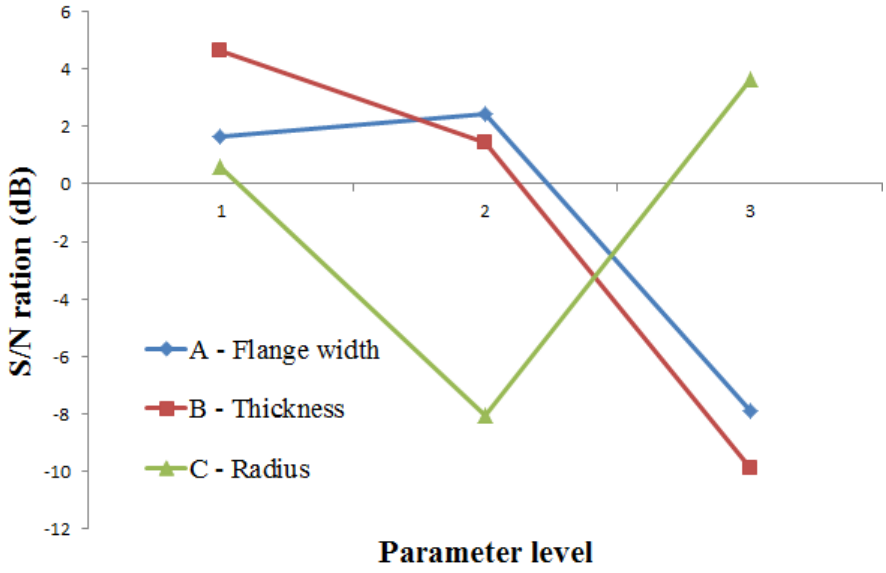

Fig 20 The parameter levels of the factors

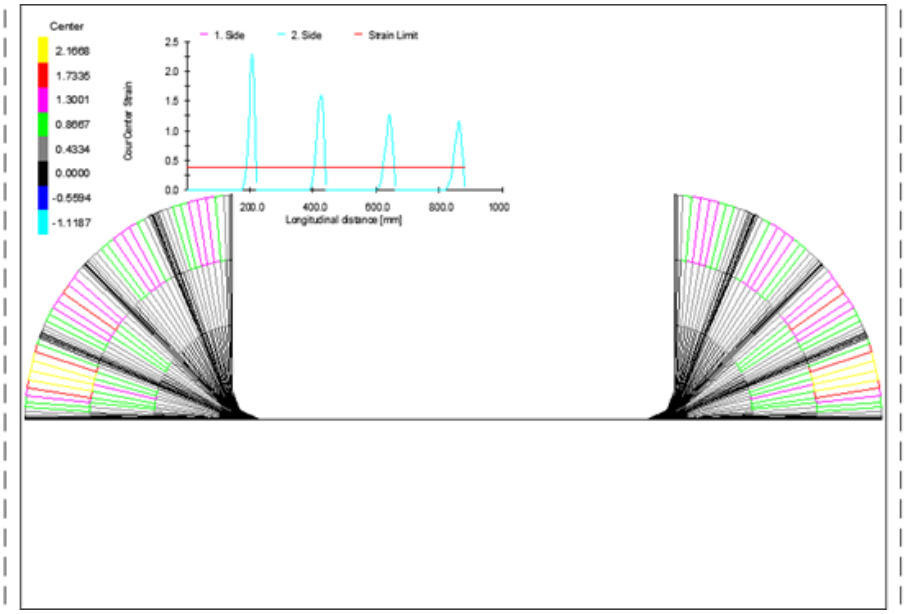

Fig. 21 The strain distribution of the sheet after roll forming process

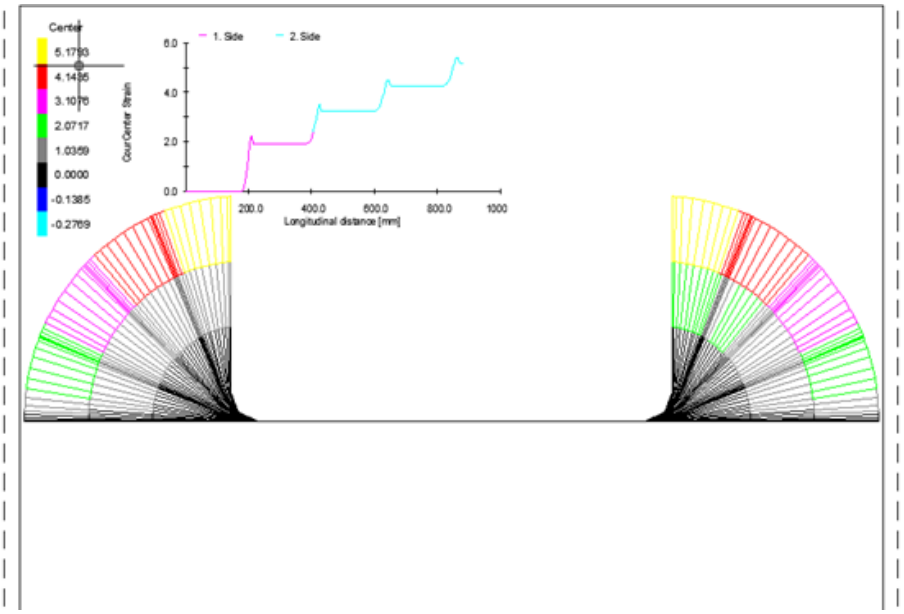

Fig. 22 The plastic strain distribution of the sheet after roll forming process

3.2 The ABAQUS simulation and experiment of spring back

The simulations with ABAQUS software have been established in the current work. The forming process is simulated by the ABAQUS/Explicit and then the result can be imported to the ABAQUS/Implicit to do the spring back simulation. The sheet passes through the roll and gets the cross-section we desired. The rolls in the simulation is considered to be rigid body and have no deformations in the forming process. The analytic rigid body used to reduce the simulation time and simplify the simulation process. There are four stages and the deformation of every stage is 22.5 degrees, 45 degrees, 67.5 degrees, 90 degrees. The distance between the rolls in roll forming direction is constant to be 220 mm. The interaction between the rolls and the sheet is determined to be surface to surface interaction. The friction is not considered in this simulation. The dimension of the sheet is 60*784 mm. The thickness of the sheet is 0.84 mm. The isotropic hardening is used in the simulation with the von mise yield criterion.

3.2.1 The spring back in ABAQUS simulation

In the roll forming process, there are two kinds of boundary conditions can be used, one is the sheet move forward driven by the friction and the other one is the sheet and rolls considered to be frictionless and make sheet pass through the roll with a certain velocity. In the current work, we used the second method to conduct the simulation. According to the research of the Q. V. Bui and J. P. Ponthot [19], the frictions in the simulation have no significant influence on the simulation result such as spring back and bowing. In the other side, the existence of friction in the simulation may affect the position accuracy of the rolls and sheet.

In the roll forming process, the spring back is one of the most important

defects of the product. The sheet after forming with a certain shape, due to the residual stress ,the sheet will continue deformation and this deformation is called spring back.

In the manufacturing industry, the over bending has been used to the design according to the experience and experiments. In this way, the spring back can be compensated.

In the current study, the ABAQUS/Implicit module and ABAQUS/Explicit module have been coupled to calculate the spring back angle. For the roll forming process, the spring back process is the dimensional shape change after the separation of the rolls and sheet. Usually spring back is caused by the linear unload. In the roll forming process, when the rolls contact with the sheet, the elastic energy have been storage by the sheet, when the forming force have been unload, the elastic energy will be released and result in the sheet dimensional recovery. So in the spring back simulation, the implicit method will be more suitable. We can get the roll forming result with the ABAQUS/Explicit and import the result into the ABAQUS/Implicit and remove the load of rolls. The explicit elements also need to change to implicit element. All boundary conditions and other extra conditions used in the explicit simulation need to be deleted and then request for the spring back result.

We assumed that the spring back here refers to the spring back after the whole roll forming process. The roll forming process is shown on the Fig. 23. Three materials included high strength steel, strainless steel and mild steel have been used in the simulations. Fig. 24 shows the mise strain of the sheet after roll forming process with high strength steel. Also Fig. 25 and Fig. 26 are the mise stress distribution of the sheet with strainless steel and mild steel. In these simulations, the rolls are considered as rigid body and have no elastic and plastic deformation. In all three simulation results, the deformations at the start point and end point have the minimum stress

distribution which due to the non-uniform force change happened. The maximum stress happened at the bending area in the deformation process. In the Fig. 24, the maximum mise stress is 655 MPa which is much bigger than the yield stress which means the plastic deformation happened. For the strainless steel and mild steel, the maximum stress also bigger than the yield stress. The flange and web zone have smaller mise stress due to the smaller deformation in those areas.

The spring back angles have been shown in Fig. 27. From which we can found that the spring back angle in the high strength steel in bigger than the other two kind of materials. Also, the maximum spring back angle happened at the start point and end point.

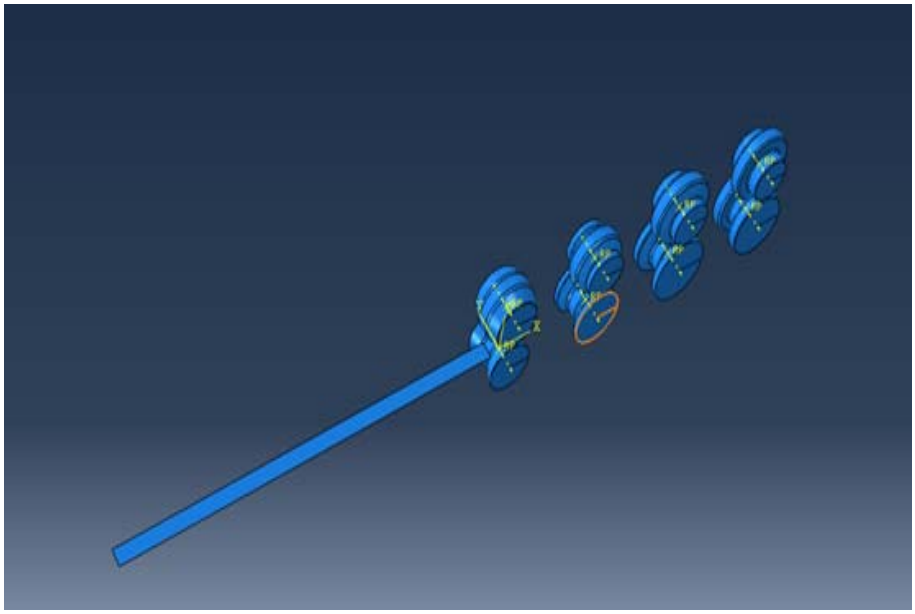

Fig. 23 The assembly of the roll forming process

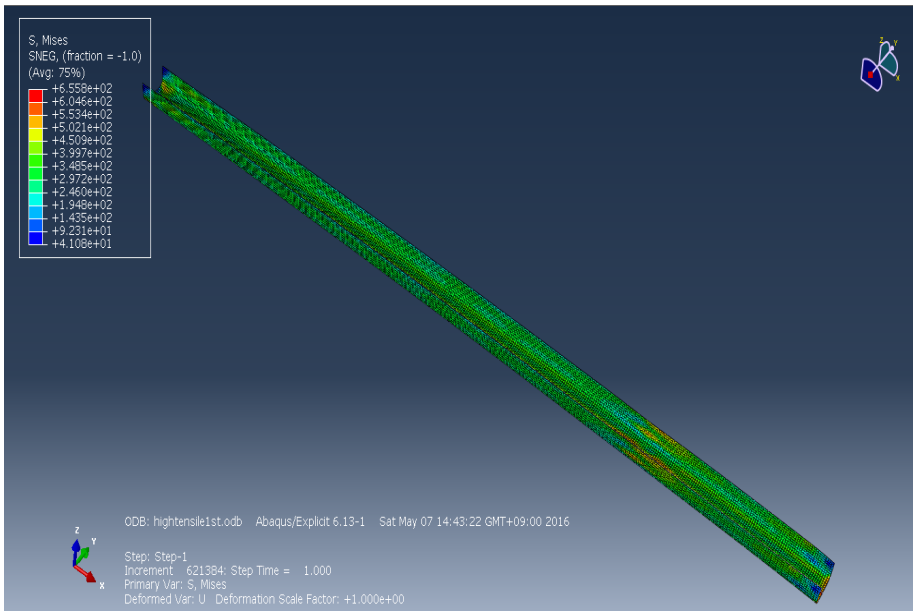

Fig. 24 The mise stress distribution of the sheet with high strength steel

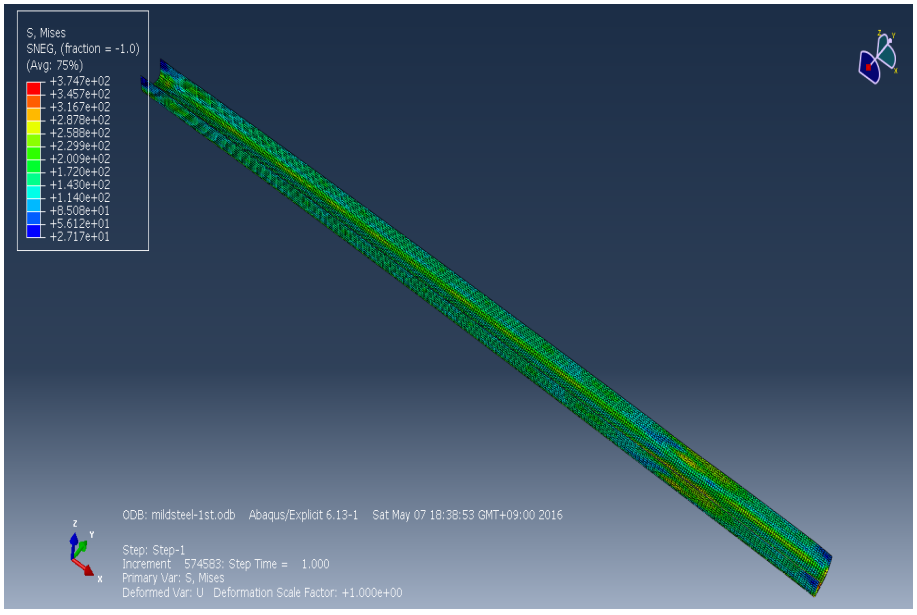

Fig. 25 The mise stress distribution of the sheet with strainless steel

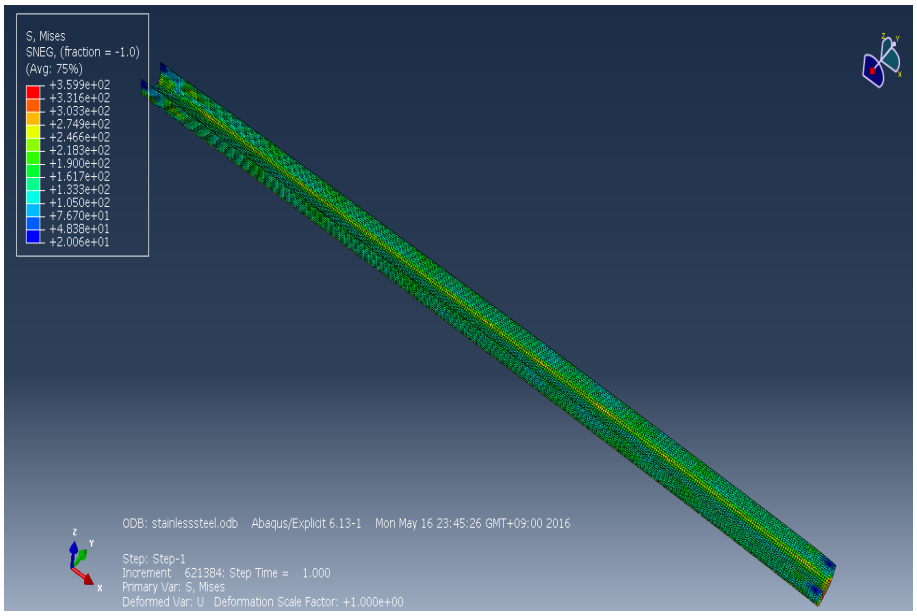

Fig. 26 The mise stress distribution of the sheet with mild steel

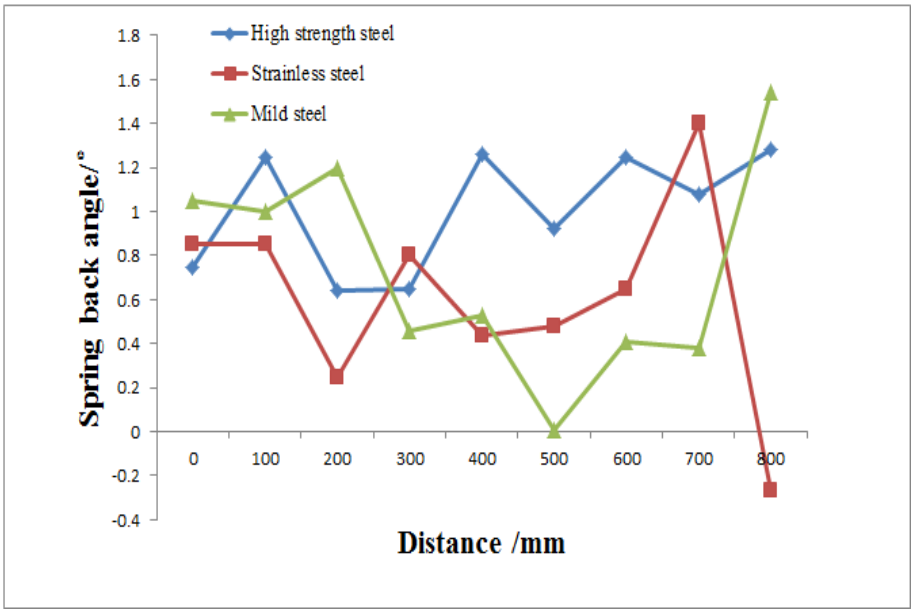

Fig. 27 The spring back angles of different materials

3.2.2 The experiment results of comparison

The experiments of roll forming with the same conditions in the simulations have been established to verify the simulation results. Fig. 28 shows the experiment results of the three materials. The spring back angle has been measured with the experiment results. We measured 9 spring back angles along the longitudinal direction of the sheet and the final spring back angle will be the average of the all measured angles.

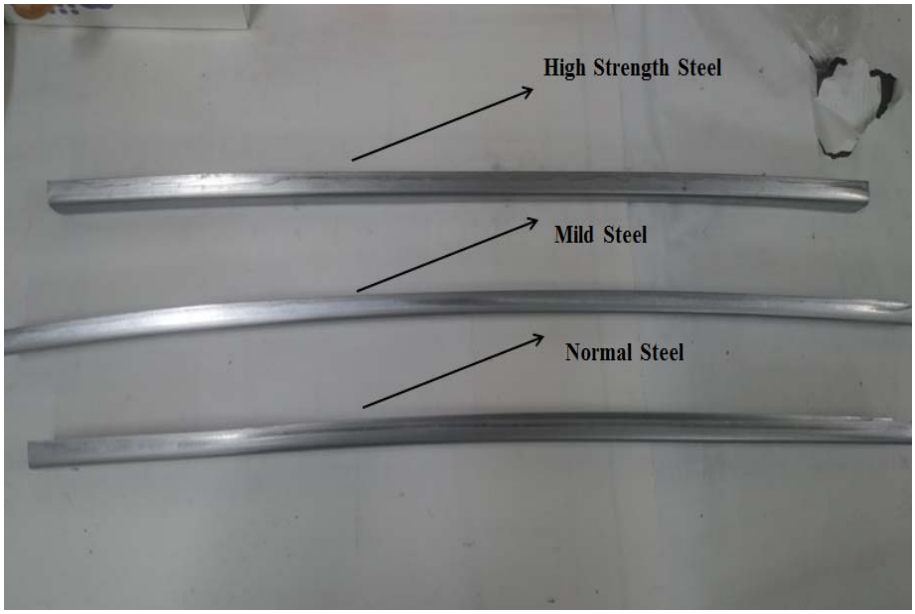

Fig. 28 The experiment results of the three kinds of materials

The spring back angles also can be calculated by the theoretical method. In this study, we used the BISWAS formula to calculate the spring back angles with three different kinds of materials. The formula can be shown as Eq. (3),

$$\frac{r_{i1}}{r_{i2}} = 1 - 1.5 * r \frac{r_{i1}}{r_f} + 0.5 * (\frac{r_{i1}}{r_{i2}})^3 \quad (3)$$

In the formula, as shown in Eq. (4),

$$r_f = \frac{E * T}{2 * S} \quad (4)$$

r_{i1} stands for the bending radius, r_{i2} is the radius after spring back, r_f is the yield curvature, E is the Young's Module, t is for the sheet thickness, S is the yield stress (Mpa).

Table 6 shows the spring back angle under experiment, simulation and theoretically calculation. From which we can know that the spring back with simulation are too small and with theoretical calculation also can not describe the spring back angle accurate. In the simulation, the material has been simplified and only a small factor has been considered. For the theoretical calculation, with the increase of forming angle, the plastic strain increased and the initial yield stress increased also. Which leads to the difference of the spring back angles.

Table 6 The comparison of spring back angles

	Simulation results (°)	Experiment results (°)	The theoretical results (°)
High Strength Steel	1.32	6.26	1.85
Strainless Steel	1.02	4.52	1.52
Mild Steel	1.13	5.94	1.50

3.3 The ABAQUS simulations of bow defect

3.3.1 The Taguchi method used in the simulation

The dimension of the sheet in this simulation is designed to be 300 mm in longitude. The sheet thickness is 0.85 mm. The material is SFPH590. The factors in the simulations are sheet width, the gap between upper roll and lower roll and the inner distance between stands. The three levels of the factors have been shown in Table 7.

Table 7 Process parameters and there levels

Symbol	Factor	Unit	Level 1	Level 2	Level 3
A	Sheet Width	mm	50	60	70
B	Gap	mm	1.5	2.0	2.5
C	Inner distance between stands	mm	170	220	270

For three levels with three factors, there will be totally 27 combinations need to be required. However, considering about the time while the effect of each factor, the orthogonal array L3 (3^3) is chosen to arrange the simulations. The combination of the simulations is listed in Table 8. There will be 9 groups of simulations with different factors and different levels.

Fig. 29 has shown the bow displacement under different conditions along the centerline of the sheet. From which we can know that the simulation 3 have the minimum bow displacement which is 0.96 mm. The simulation 4 has the maximum bow displacement which is 4.94 mm. The maximum bow displacement usually occurred in the middle of the sheet and at the end of the sheet have the minimum bow displacement.

The longitudinal strain is an important parameter in the roll forming process. Many defects are caused by the redundant longitudinal strain. Fig. 30

and Fig. 31 have shown the longitudinal strain along the edge and centerline of the sheet. We can easily find out that the longitudinal strain along the edge is much bigger that the strain along the centerline of the sheet. For both the strain along the edge and centerline are increases from simulation 1 to simulation 9. The minimum longitudinal strain along the edge will be simulation 1 and the strain is about 0.97. The minimum longitudinal strain along the centerline also is simulation 1 and the strain is about 0.39. Also for the strain at the first point and last point along the edge is much more small and the strain along the centerline are much bigger than the other point. This is because that the first point and last point have a sudden force change. This leads to the strain change at the start and the end of the forming process. Also, the data at the start point and the end point are not accurate enough. For both the strain along the edge and center line comes a maximum at simulation 9. The strain increases from simulation 1 to simulation 9.

The S/N ratio and bow displacement have been calculated in each simulation as shown in Table 9. According to the criterion “smaller is better”, the corresponded S/N ratio shows that the minimum S/N ratio is experiment 3 with A1, B3 and C3. The minimum bow displacement will be 0.96 mm.

Table 8 The orthogonal array of ABAQUS simulation

Simulation No.	Parameter Levels		
	A	B	C
	Sheet Width (mm)	Gap (mm)	The inner distance between stands (mm)
1	50	1.5	170
2	50	2.0	220
3	50	2.5	270
4	60	1.5	220
5	60	2.0	270
6	60	2.5	170
7	70	1.5	270
8	70	2.0	170
9	70	2.5	220

Table 9 Comparison of measured roughness data of bow defect

Simulation No.	Parameter Level				Calculated S/N ratio ration for bow displacement (DB)
	A (mm)	B (mm)	C (mm)	The bow displacement (mm)	
1	50	1.5	170	4.87	-13.75
2	50	2.0	220	2.15	-6.65
3	50	2.5	270	0.96	0.35
4	60	1.5	220	4.94	-13.87
5	60	2.0	270	1.45	-3.27
6	60	2.5	170	3.07	-9.74
7	70	1.5	270	2.62	-8.36
8	70	2.0	170	4.89	-13.78
9	70	2.5	220	1.87	-5.43

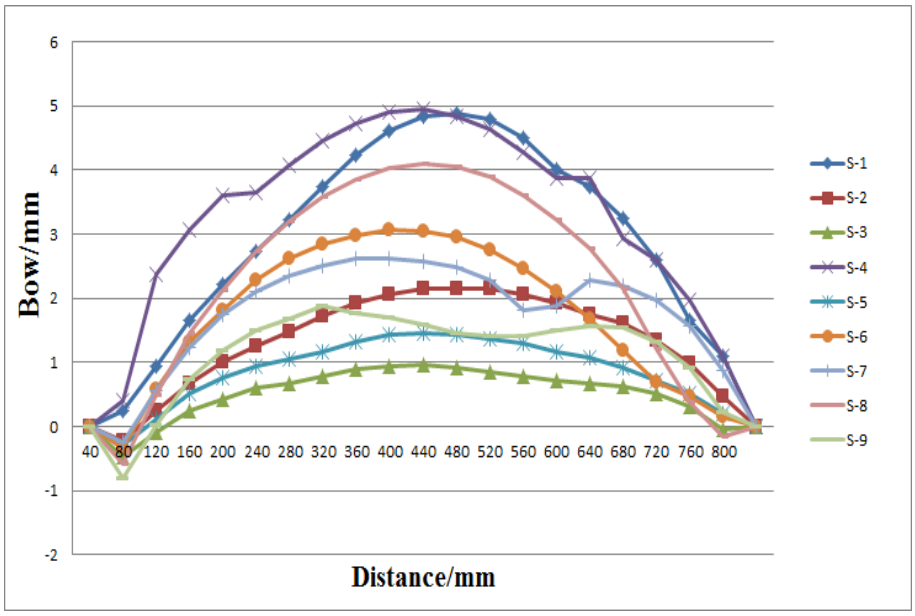

Fig. 29 The bow displacement in simulations

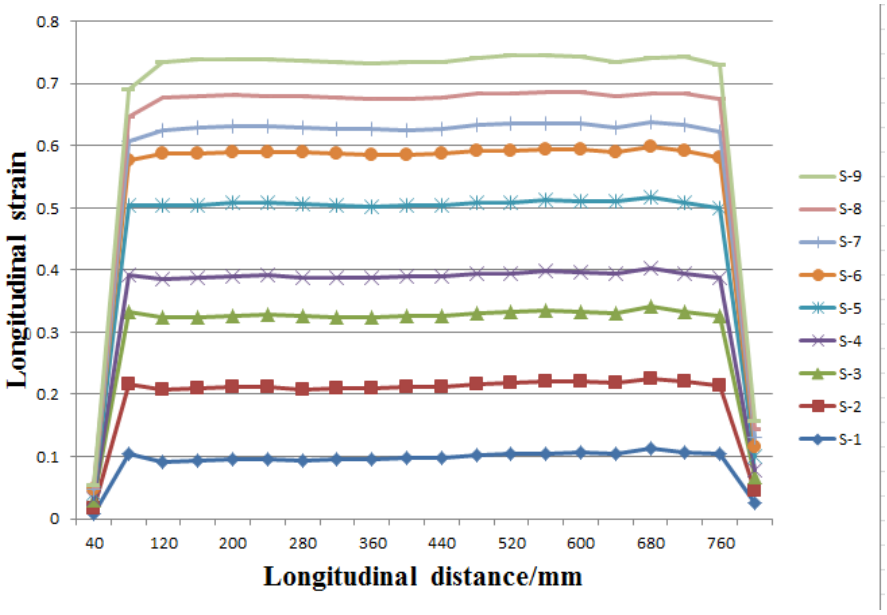

Fig. 30 The longitudinal strain along the edge of the sheet

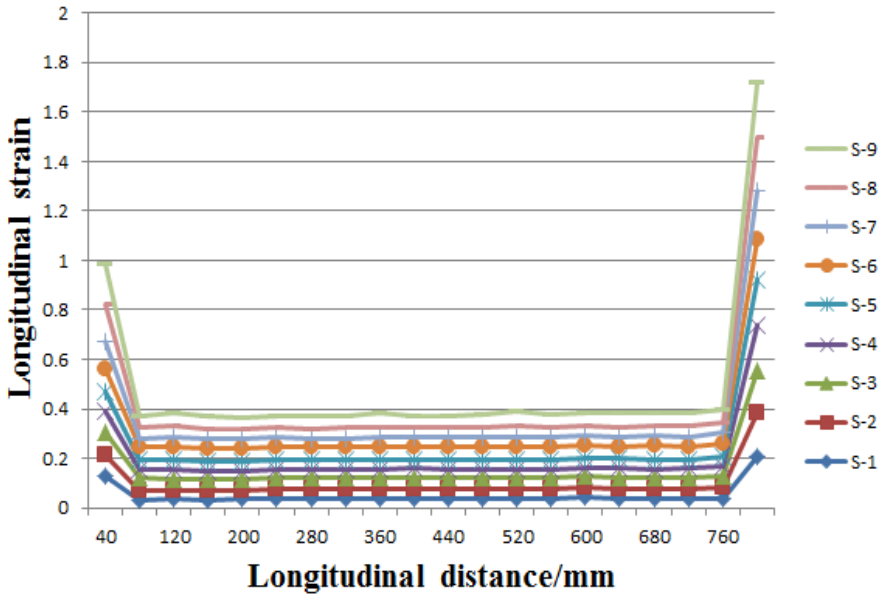

Fig. 31 The longitudinal strain along the centerline of the sheet

3.3.2 The optimization and analysis

The parameter levels of the three factors have been shown in Fig. 32. According to the rule "smaller is better", we can conclude out that the best factors for the smallest bow defect will be A1, B3 and C3. Which means the increase of sheet width will lead to a bigger bow displacement. In the other side, the gap and the inner distance between the rolls will decrease the bow displacement in some extent. The factors are same with simulation 3. The smallest bow displacement is 0.96 mm.

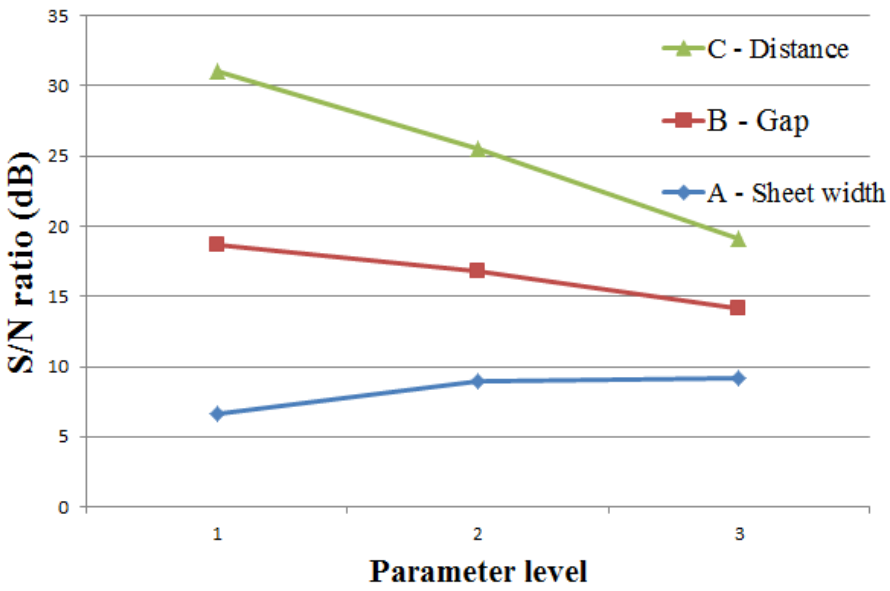

Fig. 32 The parameter levels of bow defect

3.4 The influence of pre-heating in roll forming process

3.4.1 The simulation result of pre-heating with ABAQUS

There are four simulations have been down with the ABAQUS software. The material used in the simulation is SPFH590. The temperature in the simulations have been set as room temperature, 50 ℃, 150 ℃ and 250 ℃. The spring back and bow defect have been compared with difference temperature to reveal the relation between the temperature and forming parameters.

In the simulations, we assumed that the temperature is constant and there are no any other kinds of heat transfer or heat radiation. The sheet element type will be S4R and the step time in the simulation will be 1 second. Only a half of the sheet has been considered in the simulation because of the symmetry. The friction between the roll and sheet are considered to be frictionless. The rolls are rigid body and have no any kind of deformation all around the forming process.

The simulation conditions of pre-heating are as same as with the simulation under room temperature. The sheet is model with shell element which element type is S4R. The interaction between the rolls and sheet is surface to surface interaction. The mise yield criterion has been used in the simulation. The hardening used in the simulations is isotropic hardening. Although there are many kinds of hardening modules in the ABAQUS, the isotropic hardening is the most suitable in this situation considering about the accuracy and time cost. The boundary conditions have been set by the displacement condition and the sheet is fixed, rolls pass through the sheet and deformation happened.

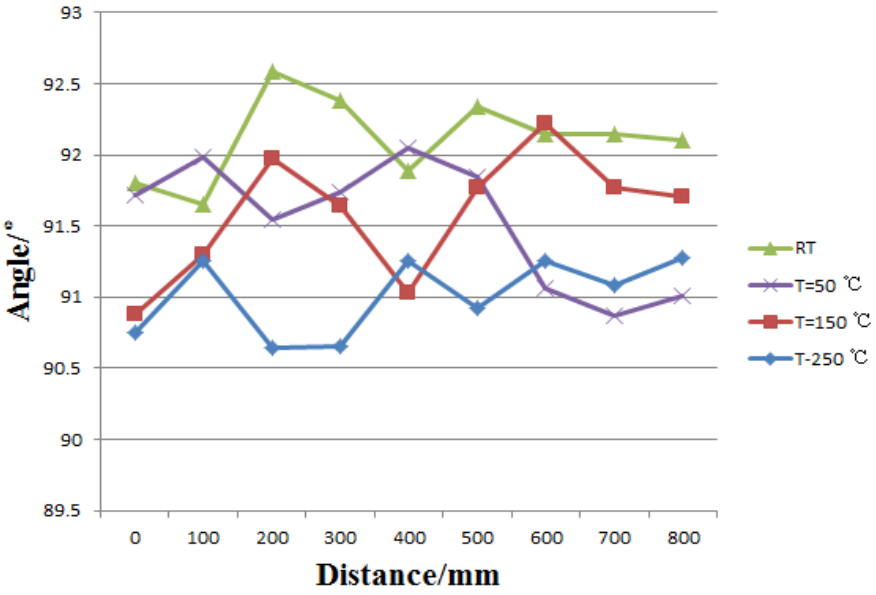

Fig. 33 The spring back angles measured in ABAQUS with different temperature

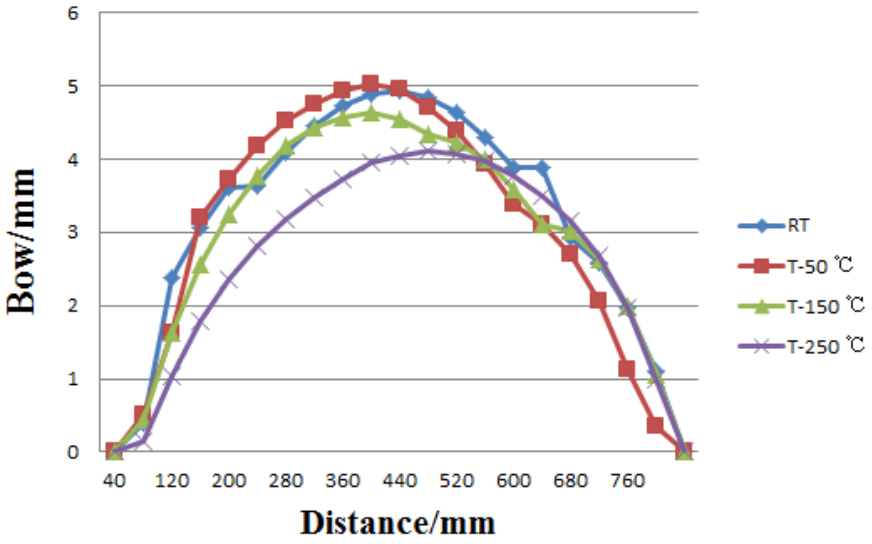

Fig. 34 The bow defect measured in ABAQUS with different temperature

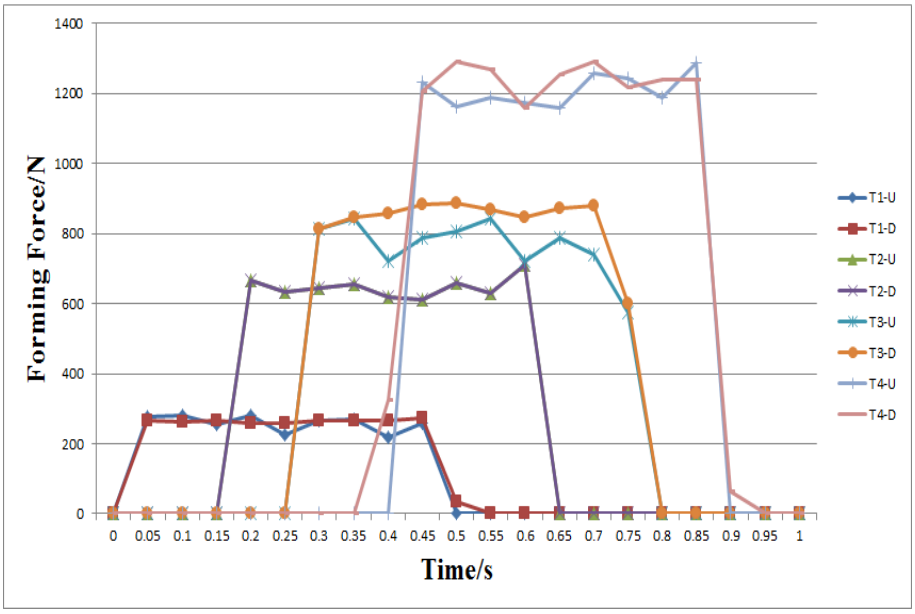

Fig. 35 The forming force under room temperature

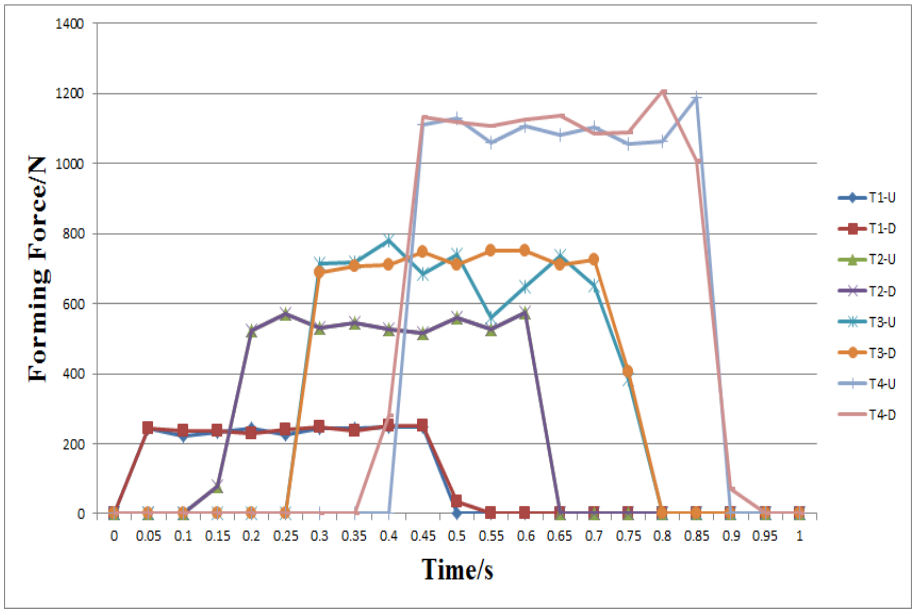

Fig. 36 The forming force under 50 ℃

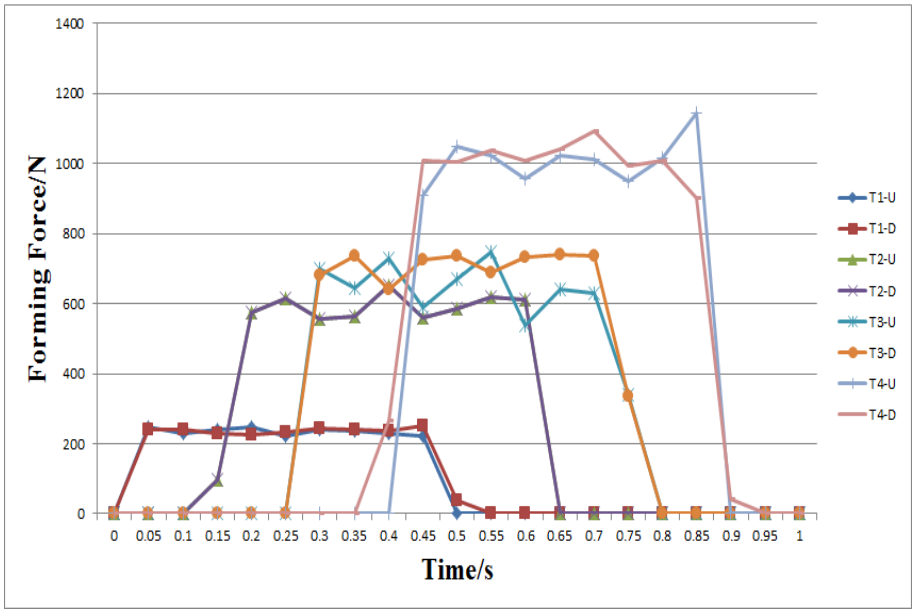

Fig. 37 The forming force under 150 ℃

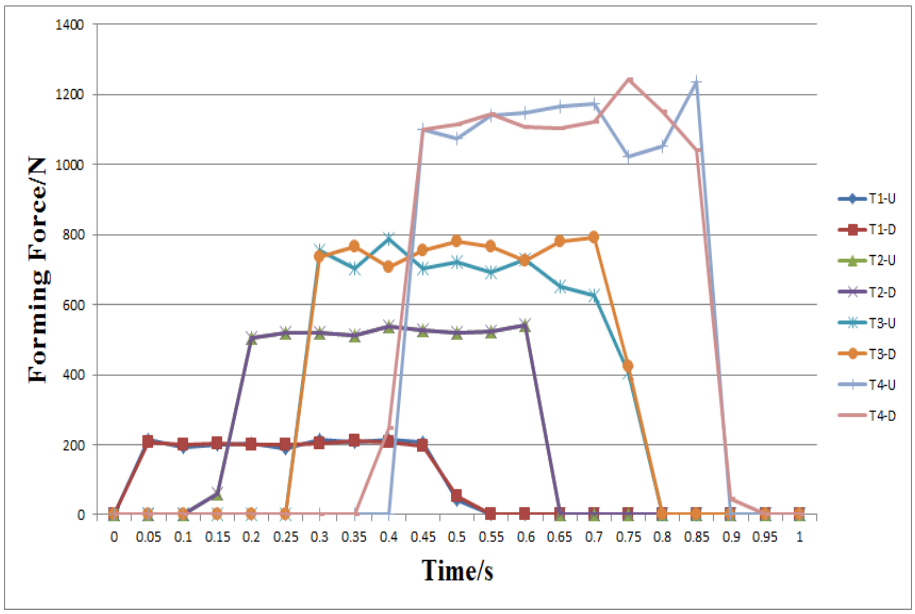

Fig. 38 The forming force under 250 ℃

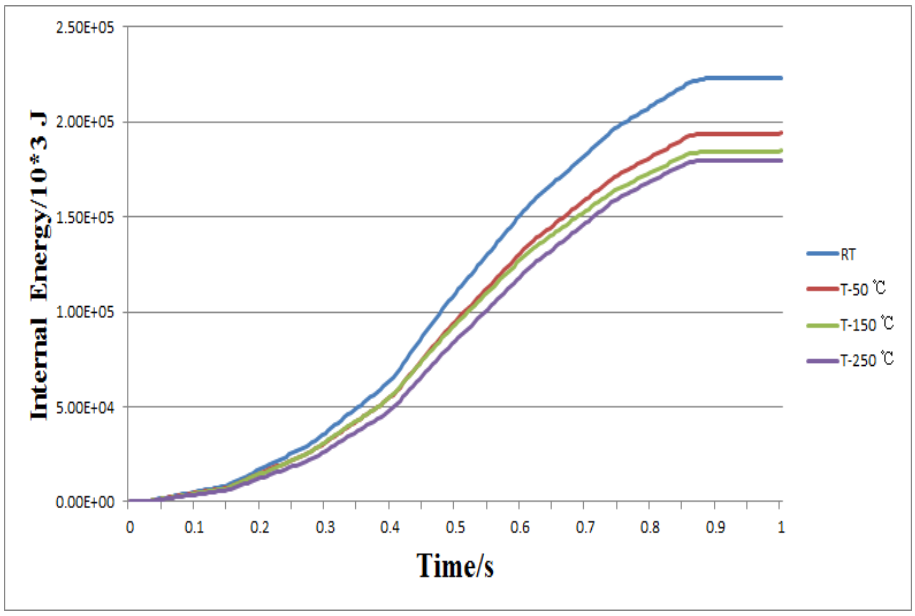

Fig. 39 The internal energy of the SPFH590 under different temperature

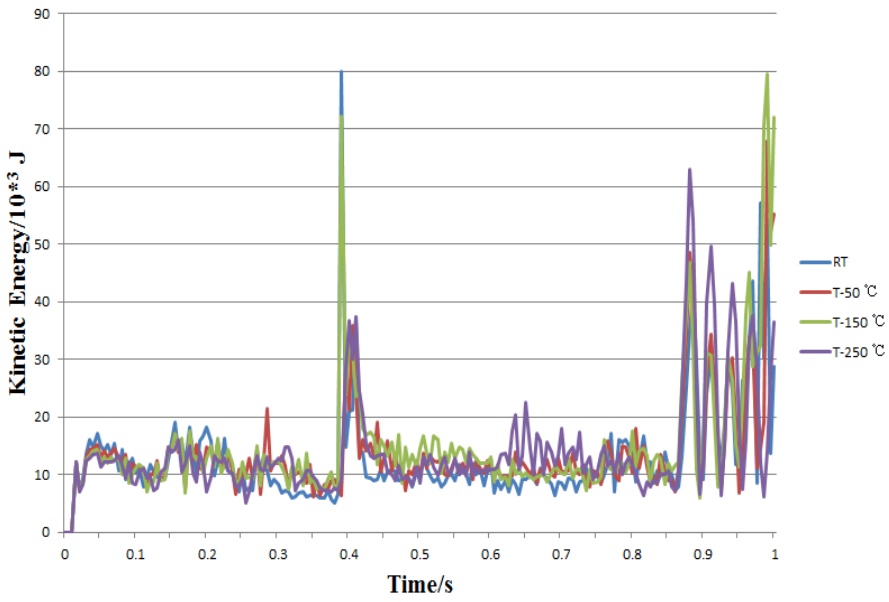

Fig. 40 The kinetic energy of the SPFH590 under different temperature

From the simulation results, we can acknowledge from Fig. 33 that the spring back angle decreases with the increasing of sheet temperature. This means the better accuracy of the sheet deformed at elevated temperature. Bow defect was measured with the displacement of the element in the center line of the sheet. The result has been shown in Fig. 34. The maximum bow displacement in room temperature is 4.94 mm. When the temperature increases to 250 ℃, the bow displacement in the same location is 4.10 mm. This means that pre-heating of the sheet can decrease the bow defect to some extent.

The forming forces of the rolls have been shown in the Fig. 35, Fig. 36, Fig. 37 and Fig. 38. The forming force of the rolls decreased with the increase of temperature. With a higher temperature, the yield strength decreased and then the forming force decreased. In general, as the temperature rises, the heat vibration amplitude between the metal atoms increased, the interatomic force decreased and result in the strength of the metal decrease (such as yield stress, ultimate strength and hardness). In the other side, the metal recovery and recapitalization happened with the high temperature, resulting in working hardening eliminated and reduce the deformation force. In some circumstances, the physical-chemical changes also have influence on the forming force. Also, we can find that the forming force of the last group is much bigger than the first group of rolls.

The kinetic energy has been shown in Fig. 40. We can know that in the simulation, kinetic energy has no significant change with different temperature. The deviation under 1 % is acceptable in the simulations. This is because the velocity in the simulation has not changed with the temperature. The internal energy which has been shown in Fig. 39 decreases with the increase of temperature. According to the energy conservation, the working by the forming force reduced with the temperature and leading to the decrease of working energy of the roll, so the internal energy decreased.

Along the forming process, the kinetic energy is smaller than 5% of the internal energy which means the simulations is reliable.

3.4.2 The experiment results of pre-heating

Depending on the requirements, pre-heating can be completed before, during, after roll forming. The experiment has been established with the butane heating. There will be 7 experiments with three kinds of steels. Fig. 41 shows the heating location use butane torch in these experiments. We can know from the Table 8 that the experiments have been done based on the different heating location. Other experiment factors are same in those experiments. The velocity of the roll, the inner distance of the roll and sheet dimension are same. The butane torch has been fixed in a frame with a height of 800 mm as shown in Fig. 42. The butane torches setting have been shown in Fig. 43. There are totally 4 torches used in the forming process and the sheet passes through the rolls from right to the left. By controlling the heating location and torch quantity we can control the experiment conditions easily. The velocity in the experiments will be 24.86 mm/s. The inner distance of the rolls is 220 mm. The thickness of the sheet is 0.82 mm and the gap between upper roll and lower roll is set to be 1 mm. The high strength sheet has a length of 746 mm and the length of the mild steel is 750 mm. The length of the strainless steel will be 810 mm. The widths of all the sheets are 60 mm.

Table 10 The experiments with pre-heating

Experiment No.	Heating Location
1	1
2	2
3	3
4	4
5	1, 2
6	1, 2, 3
7	1, 2, 3, 4

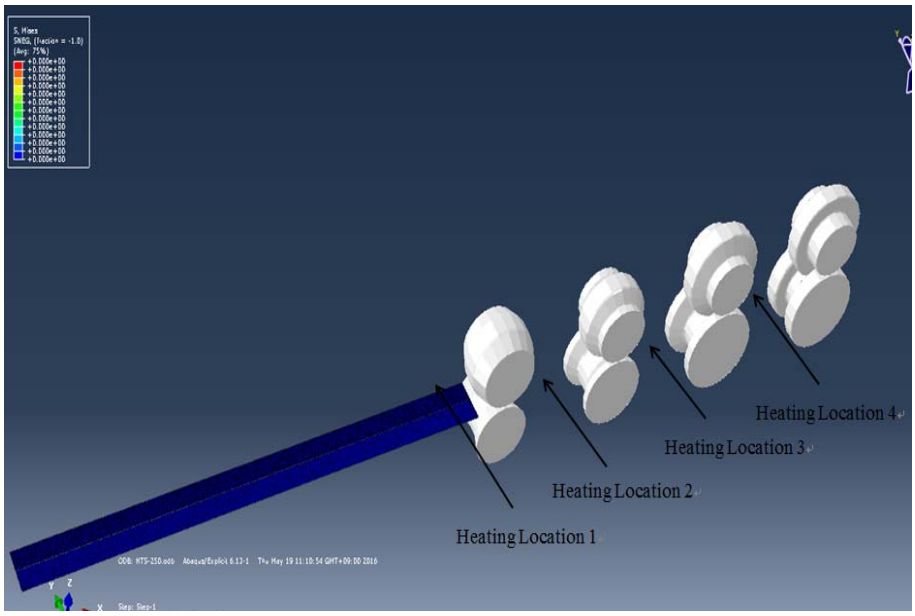

Fig. 41 The pre-heating locations of the experiments

Fig. 42 The pre-heating height of the butane torch

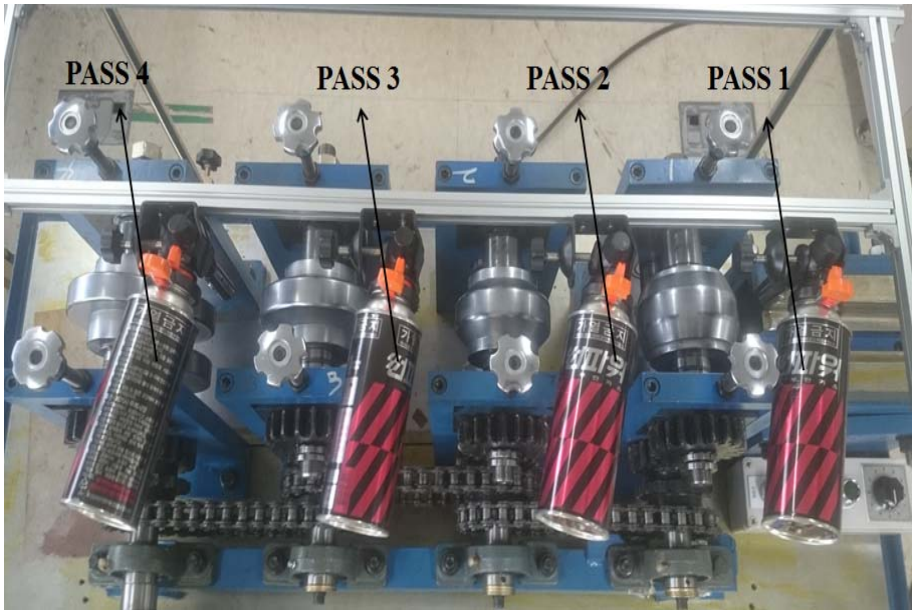

Fig. 43 The butane torch setting in the forming process

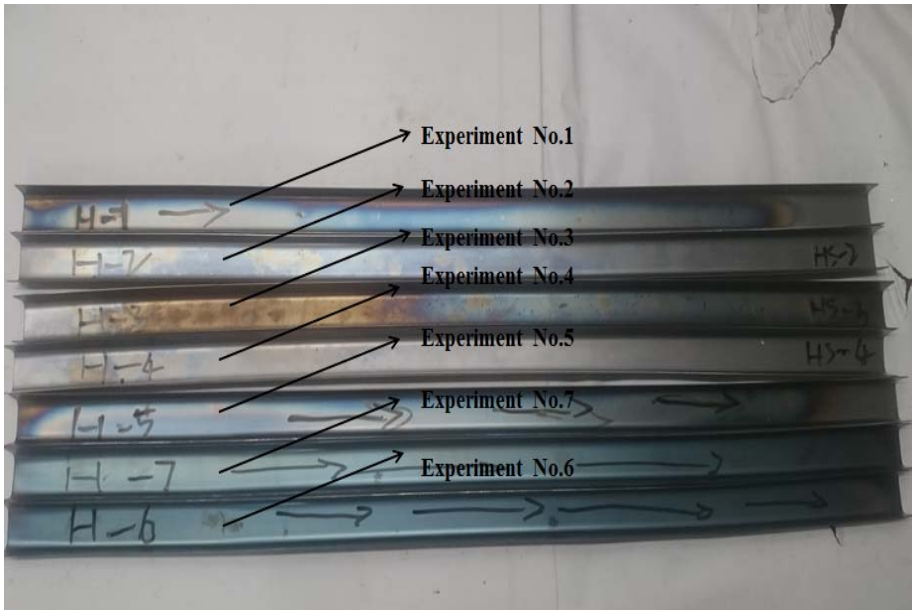

Fig. 44 The experiment results of high strength steel with pre-heating

Fig. 45 The experiment results of strainless steel with pre-heating

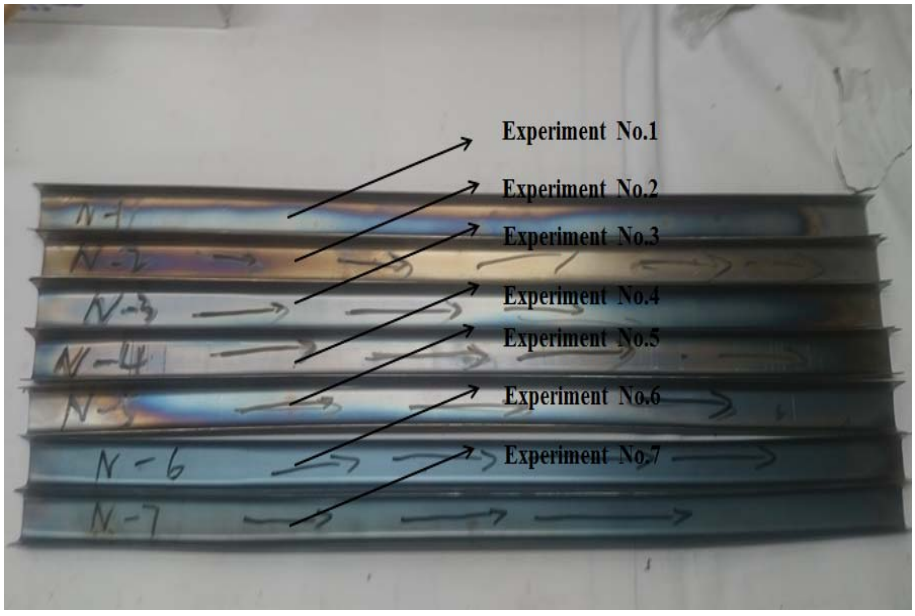

Fig. 46 The experiment results of mild steel with pre-heating

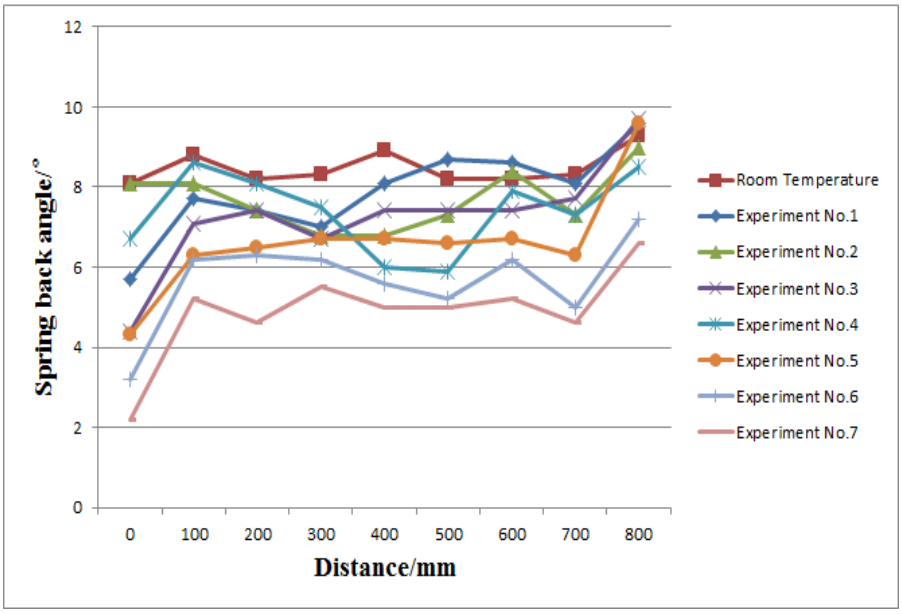

Fig. 47 The spring back angles of different pre-heating locations with high strength steel

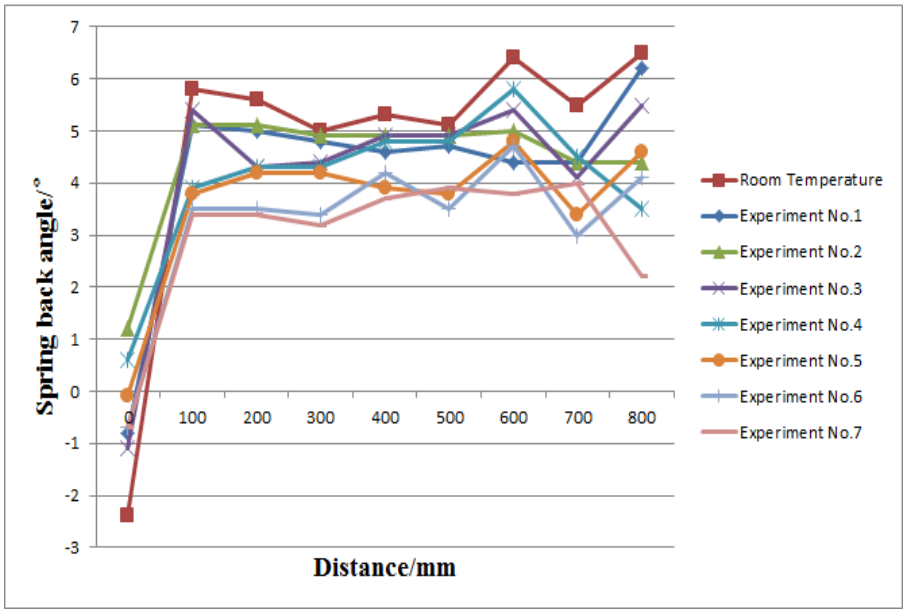

Fig. 48 The spring back angles of different pre-heating locations with strainless steel

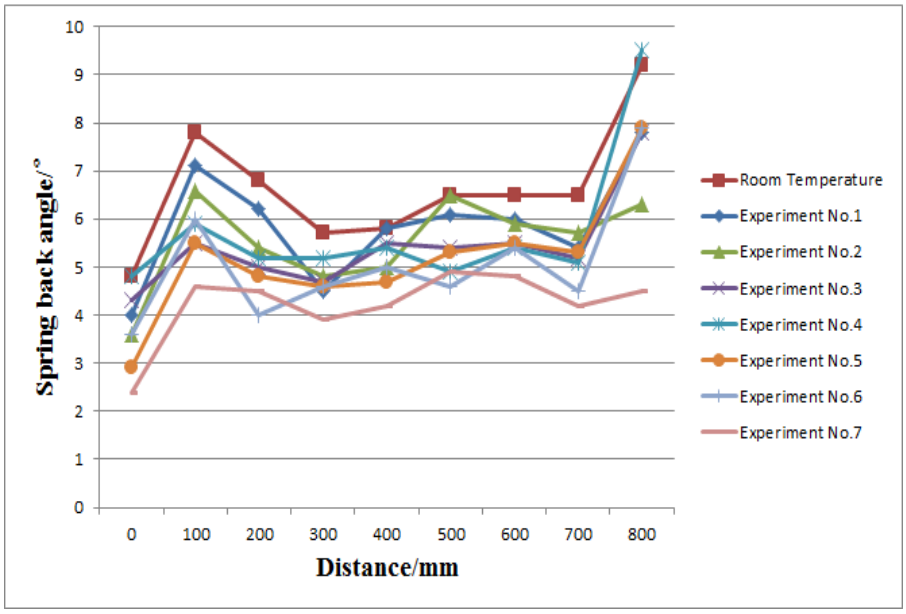

Fig. 49 The spring back angles of different pre-heating locations with mild steel

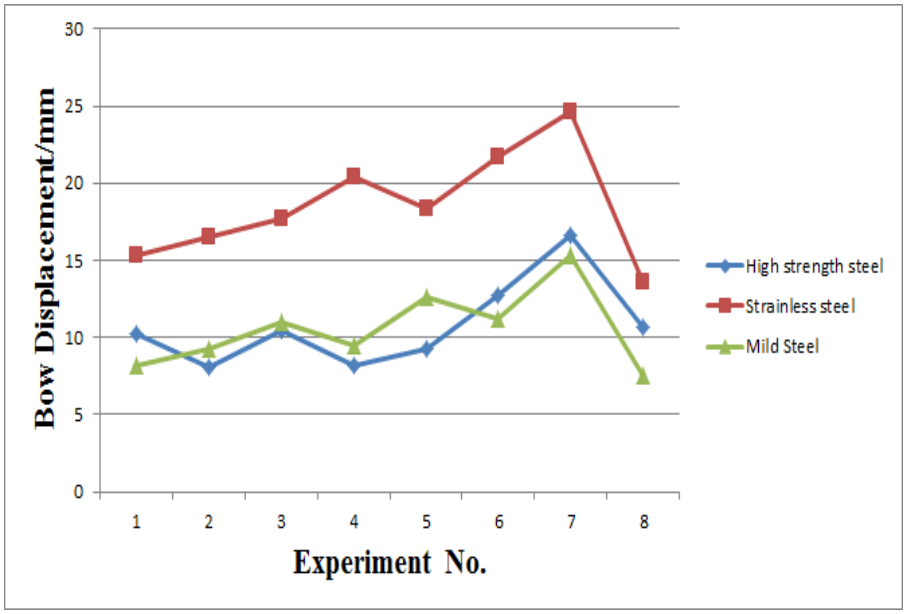

Fig. 50 The bow displacement of different materials

As schematically illustrated in Fig. 44, Fig. 45 and Fig. 46, the figures have shown the experiment results of three materials with different pre-heating method. The experiment results are acceptable and there are no big defects occurred.

Fig. 47, Fig. 48 and Fig. 49 shows spring back angles of the three materials with different pre-heating location. We can know from the figures that spring back angles in the room temperature of three materials are the biggest. The spring back angles in some experiments with the pre-heating process have a bigger spring back angle. This is may due to the deviation of the measurement of the spring back angle. In the all three materials, the spring back angles share the same tendency that the spring back angles decreases with the experiment pre-heating. With more pre-heating process and the temperature increases, the spring back angles decreased. Also, the heating positions of the sheet have no significant influence in the spring back angle. The spring back angle of different heating location have almost same spring back angles.

Fig. 50 shows the bow displacement of the sheet with different heating location of different materials. Bow displacement is affect by many factors and one of the most important factors is the tension along the edge of cross section and this tension have a tendency to make the cross section longer in the longitudinal direction. In the other side, the tension is insufficient for the whole cross section of the sheet and makes the sheet curved. We can know that the strainless steel have a bigger bow displacement compared to other two materials. For all three kinds of materials, the bow displacements become bigger with the increases of temperature. The bow displacement of mild steel is bigger than the other two kind of materials because the mild steel used in the experiment is a little longer than the other two materials.

Ⅳ. Conclusions

From the study in this paper, we have established groups of simulations and experiments to explore the influence of forming parameter on the forming results. The forming defects also have been analyzed with the Taguchi method and related factors have been optimized. The high strength steel has been used in this paper and compared with other steels. Also, the results of COPRA software and ABAQUS software have been compared with the experiment results.

We can conclude out that :

1) The factors considered in these simulations with COPRA software are not enough to cover the relationship between the spring back and forming parameters. More factors such as forming gap, forming speed and inner distance of the stands should be considered. For the factors in this study, the results show an optimal combination of the three factors A1, B2, C1 and result in the smallest spring back angle. The minimum spring back angle with Taguchi method will be 1 °.

2) The spring back simulations with ABAQUS have calculated the spring back angle with three materials. The spring back angles of the high strength steel is bigger than the other two kinds of the materials. From which we can conclude out that the yield stress can affect the spring back angles. The higher the yield stress is, the spring back angle will be bigger. The experiment results of the roll forming with these materials are much bigger than the simulation results and theoretical results. The reason is in the simulations, the materials are considered to be isotropic, homogeneous and

continuous, plane strain exits. Also, the sheet has been considered as S4R element in the simulation to save calculation time. Besides, in the theoretically calculation, the BISWAS have not considered about the forming speed and gap between the rolls and sheet. The final results need to consider about more forming factors.

3) The bow defect has been analyzed by the ABAQUS with Taguchi method. The optimization has shown the best combinations of the existed factors. The results show that a smaller sheet width will gain better result. However the other two factors are opposites, the bow displacement will increases with the gap and inner distance. The longitudinal strains along the edge and the centerline of the sheet have been calculated. The longitudinal strain along the edge is bigger than strain along the center line.

4) The influence of pre-heating has been studied with the simulation method and experiment method. The simulation results show that the pre-heating have a positive influence on the forming defects of spring back but have a negative influence on bow displacement. The forming force of the rolls decreases with the increase of temperature. The internal energy increases with the temperature.

The experiment results of the roll forming with pre-heating have the same tendency with simulation results. The spring back angles in the room temperature is bigger than the other sheets with pre-heating process in all three kinds of materials. For high strength steel, the spring back angle in experiment 7 is 34.3% smaller than the angle in room temperature. The bow displacements in the simulations are much smaller than that in the experiment which is because in the experiments, there is no any flatteners have been used. For the simulations, because of the boundary conditions, the sheet can move forward more stable. The bow displacement increases with

temperature. The maximum bow displacements are occurs in experiment 7. For high strength steel, the bow displacement in experiment 7 is 35.8% bigger than the displacement in room temperature. The simulation and experiment results can help us design and optimize the roll forming process. The results can give guidance to the roll design, optimize the forming parameters and also help to predict the metal flow.

Reference

[1] S. K. Panthi, N. Ramakrishnan, Meraj Ahmed, Shambhavi S. Singh, M. D. Goel, Finite Element Analysis of sheet metal bending process to predict the spring back, Materials and Design, Vol. 31, pp. 657 - 662, 2010.

[2] J. R. Cho, S. J. Moon, Y. H. Moon, S. S. Kang, Finite element investigation on spring-back characteristics in sheet metal U-bending process, Journal of Materials Processing Technology, Vol. 141, pp. 109 - 116, 2003.

[3] B. Shirani Bidabadi, H. Moslemi Naeini, M. Salmani Tehrani, H. Barghikar, Experimental and numerical study of bowing defects in cold roll-formed, U-channel sections, Journal of Constructional Steel Research, Vol 118, pp. 243 - 253, 2006.

[4] A. Abvabi, B. Rolfe, P. D. Hodgson, M. Weiss, The influence of residual stress on a roll forming process, International Journal of Mechanical Sciences, Vol. 10, pp. 124 - 136, 2015.

[5] Mahmoud Yaakoubi, Mounir Kchaou, Fakhreddine Dammak, Simulation of the thermo mechanical and metallurgical behavior of steels by using ABAQUS software, Computational Materials Science, Vol. 68, pp. 297 - 306, 2006.

[6] Behnam Davoodi, Behrooz Zareh-Desari, Assessment of forming parameters influencing spring-back in multi-point forming process, A

comprehensive experimental and numerical study, Materials and Design, Vol. 59, pp. 103 - 114, 2014.

[7] Xuechun Li, Yuying Yang, Yongzhi Wang, Effect of the material hardening mode on the spring back simulation accuracy of V-free bending, Journal of Materials Processing Technology, Vol. 123. pp. 209 - 211, 2002.

[8] Zhengyang Cai, Keshan Diao, Xiangdong Wu, Constitutive modeling of evolving plasticity in high strength steel sheets. International Journal of Mechanical Sciences, Vol. 107, pp. 43 - 57, 2006.

[9] M. Lindgren, Cold roll forming of a U-channel made of high strength steel, Journal of Materials Processing Technology, Vol. 186, pp.77 - 81,2007.

[10] G. Nefussi, P. Gilormini, a simplified method for the simulation of cold roll forming, International Journal of Mechanical Sciences, Vol. 35, pp. 867-787, 1993.

[11] Tao Zhou, Zhao Yang, Dong Hu, effect of final rolling speeds on the stretch formability of AZ31 alloy sheet rolled at a high temperature. Journal of Alloys and Compounds, Vol. 652, pp. 434-443, 2015.

[12] A. A. lsamhan, I. Polliinger, P. Hartely, The development of real time re-meshing technique for simulating cold-roll-forming using FE methods, Journal of Materials Processing Technology, Vol. 147, pp. 1-9, 2004.

[13] Zhang Dongjuan, Cui Zhenshan, Ruan Xueyu and Li Yuqiang, An analytical model for predicting spring back and side wall curl of sheet after U-bending, Computational Materials Science, Vol. 38, pp. 707 - 715, 2007.

[14] R. Safdarian, H. Moslemi Naeini, The effects of forming parameters on the cold roll forming of channel section, Thin-Walled Structures, Vol. 92, pp. 130 - 136, 2015.

[15] Sukmoo Hong, Seungyoon Lee, Naksoo Kim, A parametric study on forming length in roll forming, Journal of Material Processing Technology, Vol. 113, pp. 774-778, 2001.

[16] Vitalii Vorkov, Richard Aerens, Dirk Vandepitte, spring back prediction of high-strength steels in large radius air bending using finite element modeling approach, Procedia Engineering, Vol. 81, pp. 1005-1010, 2014.

[17] George. T. Halmos, Roll forming handbook. CRC Press, 2006.

[18] H. H. Le, Taguchi methods principles and practices of quality design, Gau Lih Book Co, Taiwan, 2008.

[19] Q. V. Bui, J. P. Ponthot, Numerical simulation of cold roll forming process. Journal of materials processing technology, Vol. 202, pp. 275-282, 2008.